An Investigation of the Air-Flow Pattern in the Wake of an Aerofoil of Finite Span

A. Fage and L. F. G. Simmons

Email alerting service	Receive free email alerts when new articles cite this article - sign up in the box at the top right-hand corner of the article or click **here**

VII. *An Investigation of the Air-Flow Pattern in the Wake of an Aërofoil of Finite Span.*

By A. Fage, *A.R.C.Sc.*, and L. F. G. Simmons, *B.A.*, *A.R.C.Sc.*, of the Aërodynamics Department, National Physical Laboratory.

Communicated by Prof. L. Bairstow, *F.R.S.*

Introduction.

1. The earliest physical conception of the flow in the wake of an advancing aërofoil of finite span was suggested by Lanchester,[*] who showed, from theoretical considerations, that it should comprise a layer of vorticity immediately behind the trailing edge and two general circulatory motions of opposite direction of rotation, one at each aërofoil tip. Since that time, photographs of this circulatory motion of air at the aërofoil tips have been taken by Caldwell and Fales,[†] and other experimenters[‡] have located, by direct measurement, regions of vorticity in the wake, principally behind the aërofoil tips.

The purpose of the present investigation[§] is to obtain, by precise measurements of the wind speed and direction, a more complete picture than has hitherto been available of the disturbance behind an aërofoil of finite span, and to map out the changes which occur in the extent and distribution of the vorticity in the wake as it passes down-stream. The measured vorticity is considered in relation to the circulation around the aërofoil, and from this point of view the work herein described may be regarded as a continuation of that undertaken by L. W. Bryant and D. H. Williams,[||] who confirmed experimentally the Kutta-Joukowsky relation connecting circulation and lift.

The experiments were made with an aërofoil of rectangular plan form, the ratio of span to chord being 6 : 1. Measurements of the speed and direction of the wind were made in three transverse planes behind the aërofoil, at distances 0·573, 2·0 and 13·0 chords from the trailing edge, and also in a plane 0·5 chord forward of the leading edge.

---

[*] ' Aërodynamics,' vol. 1. Also " The Aërofoil," ' Proceedings of the Institution of Automobile Engineers,' vol. 9.

[†] ' Amer. A.C.A.,' Report No. 83.

[‡] See N. A. V. Piercy, " On the Vortex Pair quickly formed by some Aërofoils," ' Journal of the Royal Aëronautical Society,' October, 1923. Also L. F. G. Simmons and E. Ower, " Note on the Application of the Vortex Theory of Aërofoils to the Prediction of Downwash," ' Aëronautical Research Committee, R. & M., 914.'

[§] The work described in this paper was carried out in the Aërodynamics Department of the National Physical Laboratory, and permission to communicate the results was kindly granted by the Aëronautical Research Committee.

[||] " An Investigation of the Flow of Air around an Aërofoil of Infinite Span," ' Phil. Trans. Roy. Soc.,' Series A, vol. 225.

Two different velocity meters, of the pressure-tube and hot-wire types respectively, were employed to obtain a completely independent check on the accuracy of the experimental observations : in general, the results obtained with these two instruments were in close agreement.

The present work provides an experimental verification of the theoretical relation given by LANCHESTER,[*] that the total strength of the vorticity leaving a semi-span of an aerofoil, as obtained by integration over a transverse plane close behind the aerofoil, is equal to the circulation around the median section : it also shows that the distribution of vorticity behind the aerofoil is closely connected with the distribution of lift along the span.

The changes in the distribution of the vorticity in the wake, as the distance behind the trailing edge increases, are illustrated in diagrams which give contour lines of equal vorticity : immediately behind the aerofoil, the vorticity is concentrated in a band which increases in depth and intensity towards the aerofoil tips ; at two chords behind, the total strength of vorticity remains unchanged, but the weak region at the centre now disappears and the distribution at the tip becomes less intense and spreads over a larger area ; at 13 chords behind it appears that the " rolling-up " of the vortex band is almost complete, and that only about 82 per cent. of the total vortex strength leaving the aerofoil has been measured.

The experiments also show that, within the limits of experimental error, the flow is irrotational at a distance 0·57 chord in front of the aerofoil and also in the regions extending beyond the tips.
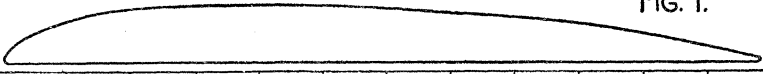
The observations show that the longitudinal velocity is *approximately* uniform over each transverse plane behind the aerofoil, so that in each of these planes the flow, relative to this longitudinal velocity, is two-dimensional, and a stream-function ψ exists. Values of ψ have been calculated, and contour lines of equal value of ψ have been drawn, and these serve to illustrate the general character of the air flow. Contour lines of equal velocity potential, determined from observations in the irrotational region of the plane two chords behind, are also included for the purpose of general interest.

Description of Experiments.

2. The aerofoil used in the experiments had a uniform section and a rectangular plan form of span 3 ft. and chord 0·5 ft. The shape of the section, known as R.A.F.6a, is given in fig. 1. The experiments were made at a wind speed of 50 ft. per second,

Section of Aerofoil.

FIG. 1.

Distance From Leading Edge.	0	0·025.	0·05	0·1	0·2	0·3	0·4	0·5	0·6	0·7	0·8	0·9	1·0
Height above Chord	0·005.	0·032.	0·044	0·060	0·074	0·076	0·075	0·071	0·065	0·057	0·044	0·027	0·005

* *Loc. cit.*

with the aërofoil mounted vertically, at an incidence of 6° to the direction of the undisturbed wind.

The aërofoil was supported on a wooden slider which was capable of movement between parallel transverse guides attached to the roof of the wind tunnel. The velocity meter was constrained to move along a fixed vertical line in the centre of the tunnel. The observations in each transverse plane were made by traversing the velocity meter along this fixed vertical line, and placing the aërofoil at different positions across the tunnel : an alteration of the plane of exploration involved a re-adjustment of the position of the aërofoil slider and guides on the tunnel roof.

Observations of wind speed and direction were made in four transverse planes, at distances 0·573, 2·0 and 13 chords behind the trailing edge of the aërofoil and 0·51 chord forward of the leading edge. The field of exploration at two chords covered a large rectangular area, which extended from the line of symmetry to a distance of 1·5 chords beyond the aërofoil tip, and vertically from 1·33 chords above to 1·225 chords below the aërofoil. The observations at the other sections were taken over a smaller field, equal in length, but having an average depth of about one chord.

3. The observations were taken with two velocity meters of different types. The first instrument was the standard speed-and-direction meter* of the Aërodynamics Department, and involves the measurement of pressure ; the second was of more recent development, and depends on the cooling effect of an air current on hot wires of small diameter. Photographs of the two instruments are given in fig. 2. Each speed-and-direction meter was mounted so that both its attitude and position could be varied and measured from outside the wind tunnel. A general arrangement of this apparatus, showing a pressure-tube instrument in place, is given in fig. 3.

FIG. 2.

To take observations, the pressure-tube instrument is rotated about vertical and horizontal axes until the pressures in each pair of tubes are equal ; the angular displacements from the zero position in the undisturbed wind then give a measure of the direction of the stream, whilst the wind speed is determined from the difference of pressure between one of these four tubes comprising the head and a fifth tube, which is shielded by a cone pointing into the wind direction.

The hot-wire instrument, previously described by L. F. G. SIMMONS,† consists of three
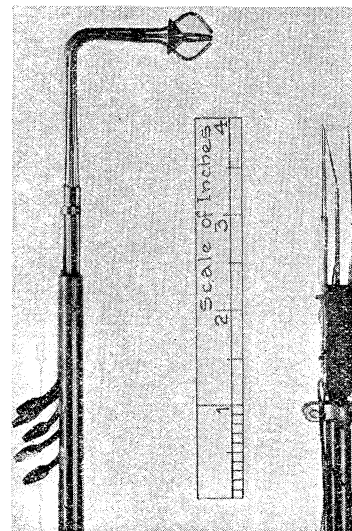
---

* " A Direction and Velocity Meter for Use in Wind-Tunnel Work," by T. LAVENDER. ' R. and M., No. 844, Aëronautical Research Committee.'

† " A Hot-wire Speed and Direction Meter," ' Aëronautical Research Committee, T 2033.'
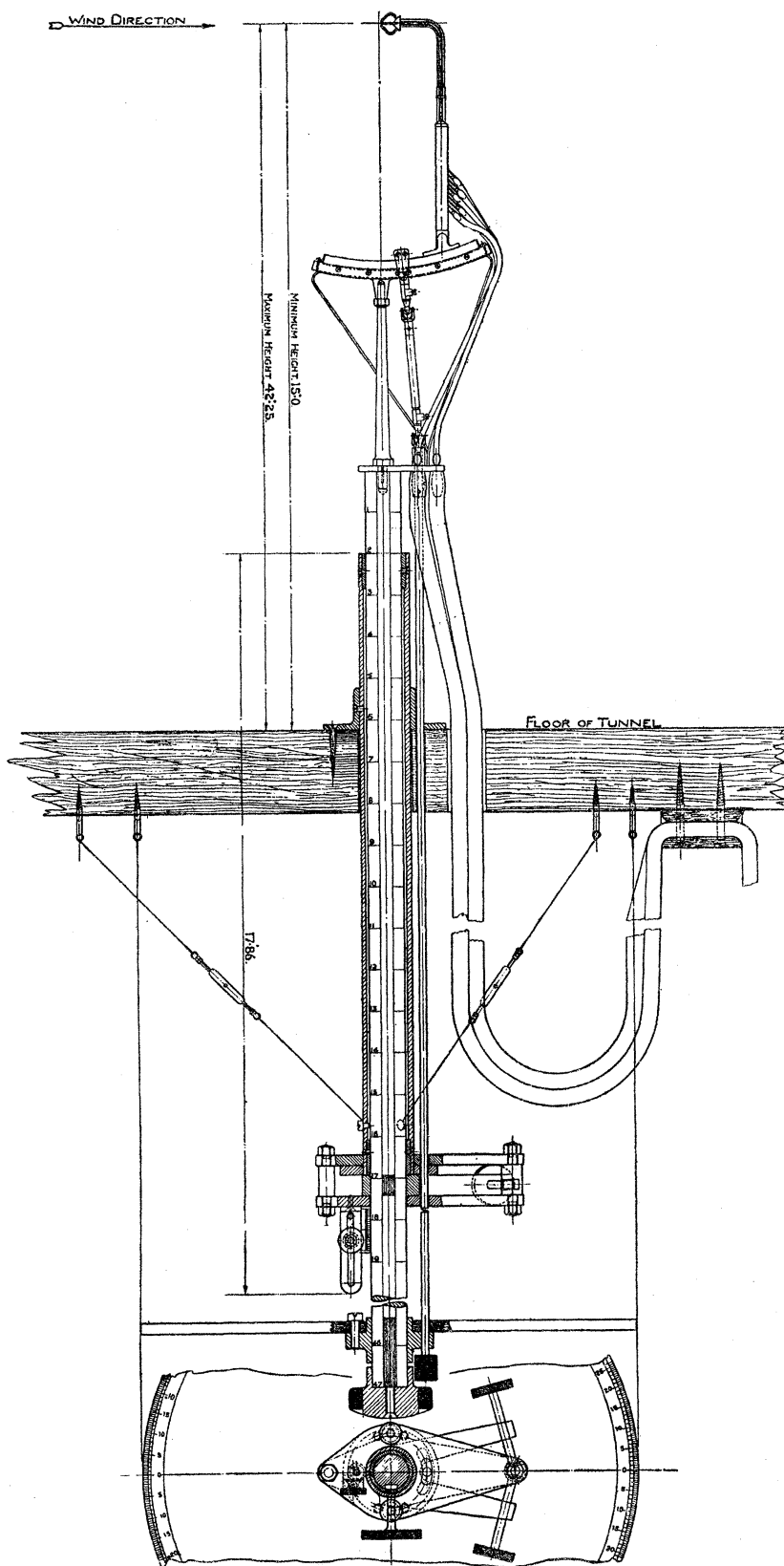
FIG. 3.

very fine platinum wires, inclined at a small angle to each other and meeting at the apex of a cone pointing up-stream.   Two of these wires are in a plane inclined upwards at 5° to the horizontal, whilst the third wire, in the vertical plane of symmetry, is inclined downwards at the same angle.   Pairs of the wires are selected, in turn, to form the opposite arms of a Wheatstone bridge, and the instrument is rotated about vertical and horizontal axes until the bridge is balanced for a given current through the wires. In this position the wires are symmetrically inclined to the air flow, and the orientation of the instrument from its position in the free stream is a measure of the direction of the flow.   The wind speed is determined by measuring the current required to keep the two lower wires at a constant excess temperature above that of the surrounding air. The instrument was calibrated before and after each set of observations, in order to take account of atmospheric changes of temperature.

Forces on Aërofoil.

4. Two independent measurements of the lift and drag on a model aerofoil of this section had been previously made at the Laboratory.*   The values for the aërofoil at an incidence of 6° and in a wind speed of 50 ft. were $K_L = 0.370$ and 0.366 and $K_D = 0.0208$ and 0.0205 respectively, where K_L and K_D are non-dimensional co-efficients of lift and drag respectively, obtained by dividing the measured forces by the product of the air density, the area of the aërofoil, and the square of the wind speed. As the agreement between these sets of values is very satisfactory, the mean values (i.e., $K_L = 0.368$ and $K_D = 0.0206$) were taken for the purposes of the present paper, and no repeat measurements were made.

The distribution of lift along the aërofoil was not measured directly, but has been estimated from the results of earlier experiments† ; these results relate to an aërofoil closely resembling R.A.F.6a, except for a slight curvature of the undersurface and a small increased camber.   It is anticipated that no appreciable error will be introduced by this procedure.

A theoretical distribution of lift has also been derived by an application, due to TREFFTZ, of the PRANDTL theory of aërofoils.‡   The two sets of results are given in Table I ; it will be seen that good agreement obtains over the greater part of the span, between the theoretical and experimental values.

---

* " Experiments at the National Physical Laboratory on the Variation of the Forces and Moments on an Aërofoil as the Speed Changes," ' R. and M., No. 148, Aëronautical Research Committee.'

† " An Investigation of the Distribution of Pressure over the entire Surface of an Aërofoil," by B. MELVILL JONES, B.A., and C. J. PATERSON, B.Sc., ' R. and M., No. 73, Aëronautical Research Committee.'

‡ " A Method of Calculating the Characteristics of a Tapered Wing," by H. GLAUERT, ' R. and M., No. 824, Aëronautical Research Committee.'   Cf. " On the Theory of Tapered Aërofoils,' by A. FAGE, ' R. and M., No. 806, Aëronautical Research Committee.'

TABLE I.—Angle of Incidence 6°. (K_L for complete aërofoil $= 0\cdot368$.)

y Chords.	Values of K_L.	
	From Experiment.	From Theory.
0	——	0
0·033	0·232	0·080
0·167	0·203	0·219
0·50	0·281	0·318
1·0	0·364	0·373
1·5	0·401	0·400
2·0	0·413	0·412
Median 3·0 Section	0·415	0·420

Experimental Results.

5. The experimental observations have been referred to the standard right-handed system of rectangular axes, OX, OY, and OZ, commonly employed for a horizontal aërofoil, and shown in fig. 4.   Contrary to the usual convention, however, the origin, O, is taken *at the aërofoil tip*, at one end of the trailing edge.   Thus, the sign of y denotes whether the point is within or beyond the aërofoil tip, and the origin is in the neighbourhood where the disturbance of flow is a maximum.

FIG. 4.

$\dfrac{\text{Span}}{\text{Chord}} = 6\cdot0$
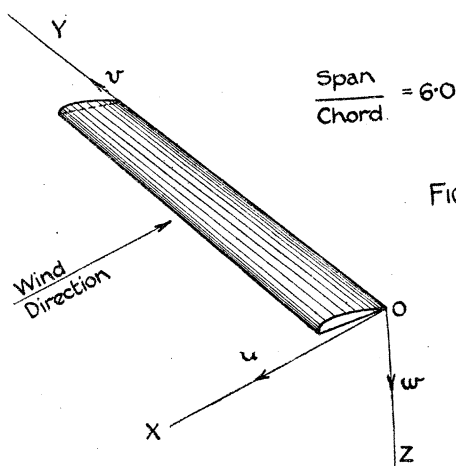
All the experimental results are given in terms of the three velocity components u, v, and w, relating to directions parallel to the axes OX, OY, and OZ, respectively. These components are expressed as absolute coefficients, the velocity of the undisturbed air, 50 ft. per second, being taken as unity.   A small correction has been applied to the values measured at the section 13 chords behind the aërofoil, to allow for the acceleration of the air down the tunnel.   Throughout the report the chord is taken as the unit of length.

For convenience, the fields of exploration will be referred to as Sections A, B, C, and D. Section A is forward of the leading edge at a distance $0\cdot51$ chord, and sections B, C, and D behind the trailing edge at distances $0\cdot573$, 2 and 13 chords respectively.

6. The general characteristics of the experimental results, for both velocity meters, are exhibited in fig. 5, where values of u, v, and w, at constant values of z, are plotted against y.   These curves are representative of the results obtained from the explorations taken along lines parallel to the trailing edge ; they include observations in the

region of intense vorticity at the aërofoil tip ($y = 0·12$ and $z = -0·088$, for this particular section), and both above and below this region.   A comparison of the observations taken with the two meters shows that the agreement on both v and w is very close,
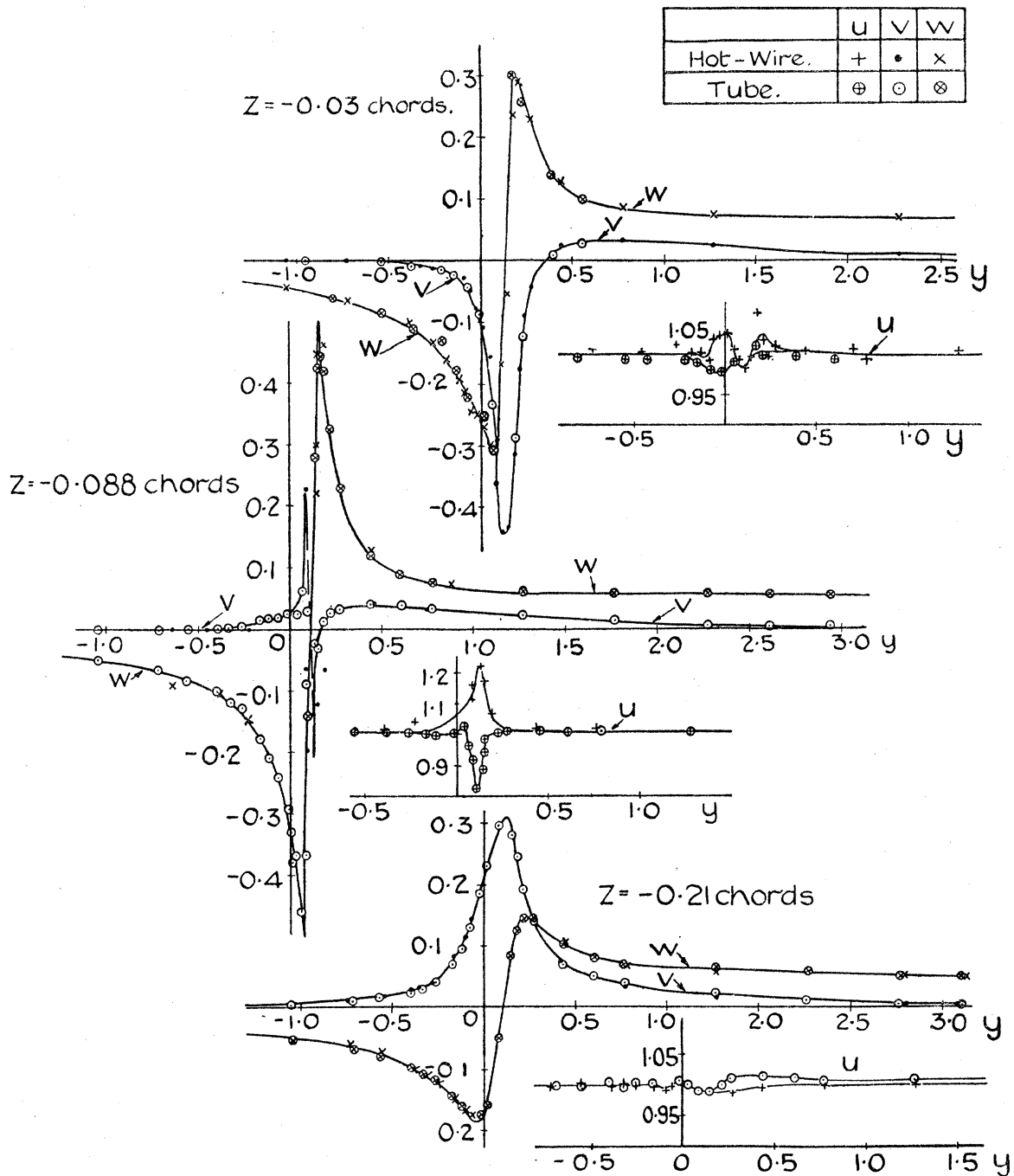
FIG. 5.—Comparison of Observations taken with Hot-wire and Tube Meters.

even in the violently disturbed region behind the aërofoil tip.   Good agreement (within 1 per cent.) also exists between the values of u, except over the small area in the

immediate neighbourhood of the vortex " core," where the observations taken with the hot-wire meter are higher than those taken with the tube meter.   It should be remarked that in this small region markedly large gradients of both speed and direction occur, so that, by reason of the comparatively large size of the meters employed, both sets of observations are open to doubt.   Apart from probable discrepancies in the vortex " core," the comparison shows that the accuracy of experimental observation is very satisfactory.

Fig. 5 also shows that the experimental observations lie evenly on well-defined curves. As this was a characteristic common to all the measurements, it was considered unnecessary to give the whole of the actual observations, but only a selection of values sufficient to define completely the shape of the experimental curves.   These results are given in the appended tables (VI—IX).

7. To illustrate some general characteristics of the flow in the wake, contour lines of equal values of v and w for Section C are given in figs. 6 and 7.   These diagrams show
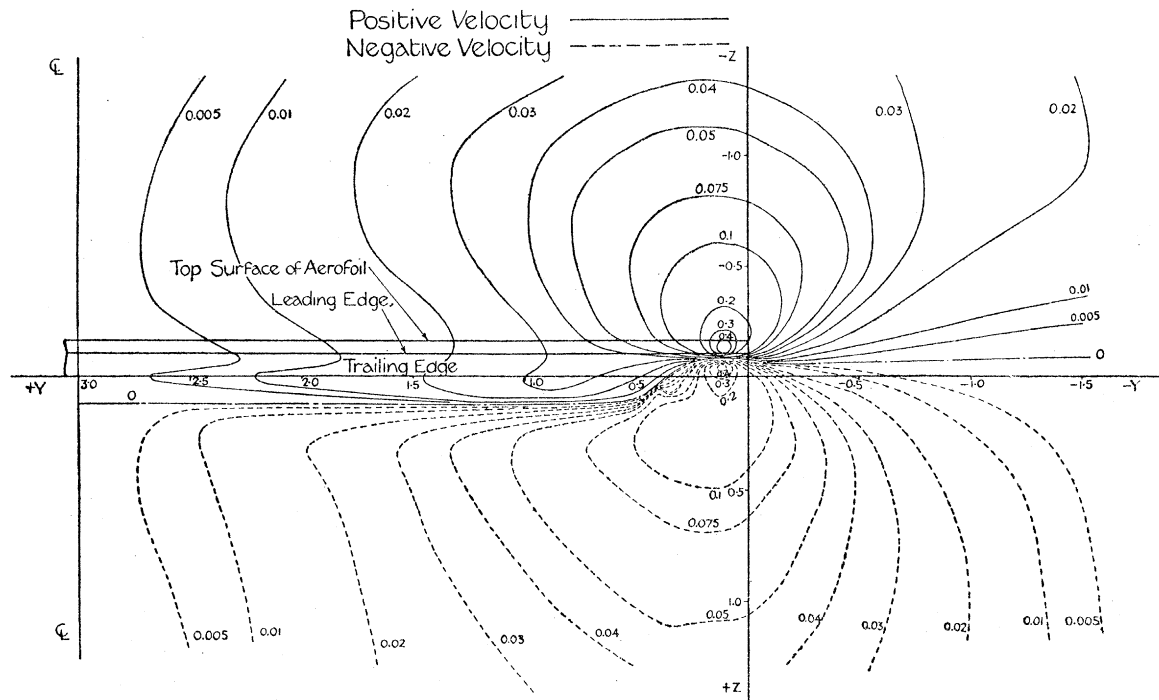
Fig. 6.—Section C (two chords behind).   Contours of Equal Horizontal Velocity Component (v).

that there is a general circulatory motion of air from beneath to above the aërofoil. Fig. 6 shows that the lateral velocity v has an outward direction below and an inward direction above the aërofoil, and also that its magnitude changes most rapidly in the neighbourhood of the contour line $v = 0$.   A detailed consideration of the flow in this region is given later.

In the near neighbourhood of the aërofoil tip ($y = 0\cdot12$, $z = -0\cdot088$) there are very steep gradients of both v and w, and the flow here closely approximates to that of a RANKINE vortex.   It is of interest to note the unevenness in the contour lines of v and w
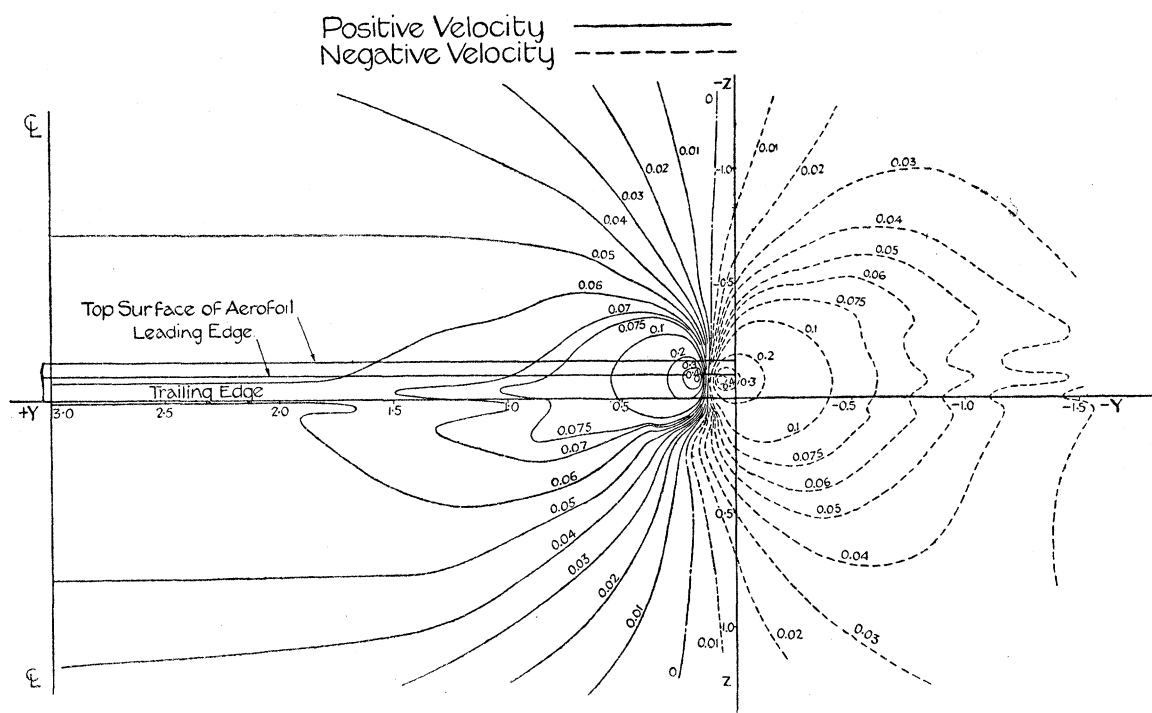
FIG. 7.—Section C (two chords behind).   Contours of Equal Vertical Velocity Component (w).

immediately behind the aërofoil, this being possibly a phenomenon associated with the profile drag.

Contour lines of v and w have not been drawn for Sections B and D, because their characteristics are similar to those of Section C.   The flow in these sections is considered later, in the sections dealing with vorticity and the streamline function ψ (§§10–15,18–20).

8. No diagrams of v and w have been drawn for the forward plane of exploration, because the observations given in Table VI indicate sufficiently clearly the character of the flow.   They show that there is a general upwash extending from the centre, where the value is a maximum, to well outside the aërofoil tip, and also that there is a small outward velocity at the tip.

9. The variations of the forward velocity u within the aërofoil wake were small (that is, within 1 per cent.), except in the small regions of intense vorticity, where the observations are of doubtful accuracy, and in front of the aërofoil.   For this reason no curves showing the variation of u behind the aërofoil are presented.   Generally speaking, the values of u above the aërofoil $(-z)$ tend to be slightly greater than those below.

The Vorticity in the Wake.

10. It is now proposed to consider the distributions of the longitudinal component of vorticity over each (y, z) plane of exploration.   The magnitude of this component is given by $\left(\dfrac{\partial w}{\partial y} - \dfrac{\partial v}{\partial z}\right)$, and has been calculated from the slopes of tangents drawn to curves of w and v plotted on y and z bases respectively.   It will be shown later that this

312   MESSRS. A. FAGE AND L. F. G. SIMMONS ON AN INVESTIGATION OF THE

process of graphical differentiation is sufficiently accurate for the present purpose. The distribution of this vorticity component over each of the Sections B, C, and D is shown by contours in fig. 8. Referring to the diagram for Section B, we see that, at about 0·6 chord behind the aërofoil, the vorticity is confined to a narrow band extending along the span, and that both the depth of this band and the intensity of the vorticity increase
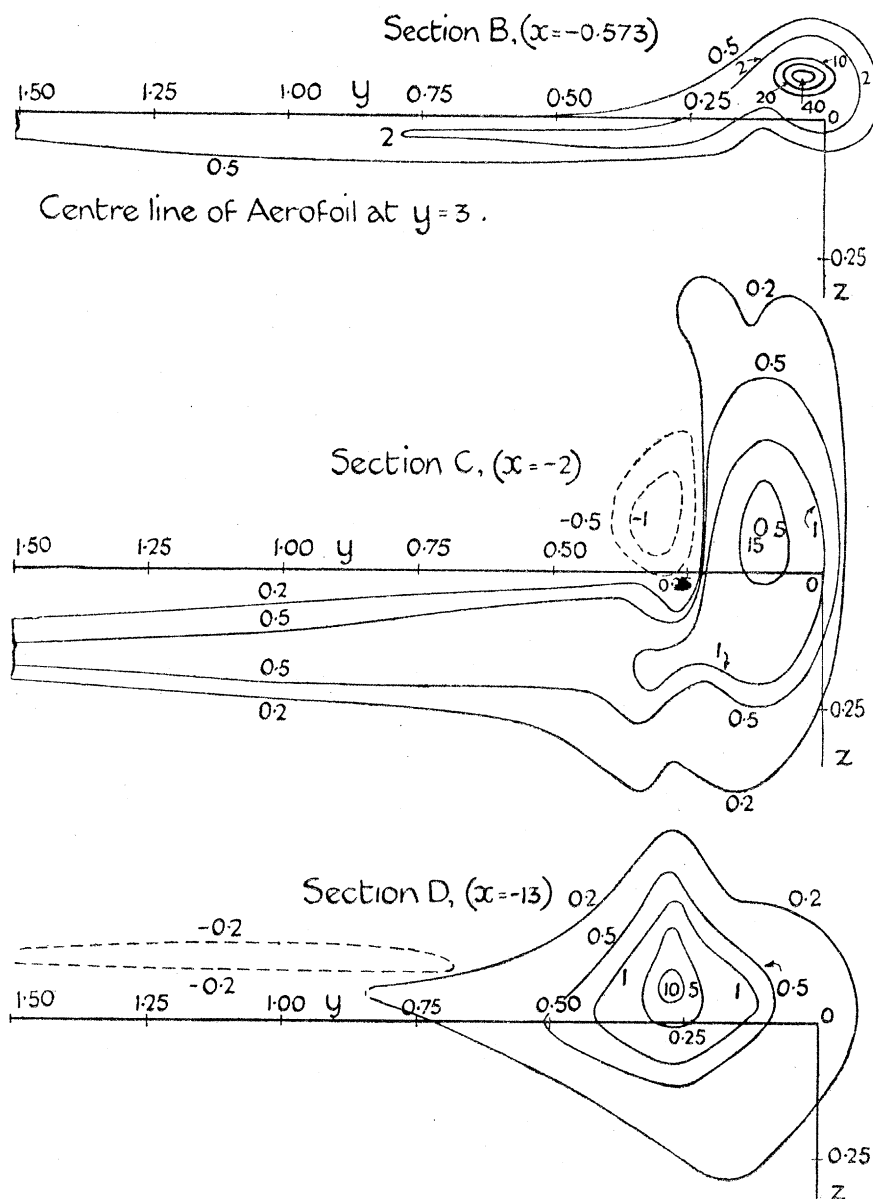
FIG. 8.—Contours of Equal Vorticity $\left(\dfrac{\partial w}{\partial y} - \dfrac{\partial v}{\partial z}\right)$.

towards the aërofoil tip. Further from the aërofoil (Section C, $x = -2$ chords) the band changes its shape and becomes narrower at the centre and deeper at the tip, whilst the vorticity at the tip, although extending over a larger area, becomes less intense. These changes demonstrate the unstable character and consequent " rolling up " of the vortex

system postulated in the PRANDTL theory. At a still greater distance behind the aërofoil (Section D, $x = -13$ chords) the "rolling-up" of the band appears to be almost complete, and practically all the vorticity is confined to a region at the tip, extending over about a quarter of the semi-span. There is some evidence of the existence of weak areas of negative vorticity at Sections C and D, although further precise measurements are required before these regions can be regarded as definitely established.

Another interesting feature exhibited in the diagrams is that the band, prior to "rolling up," follows the general direction of downwash, whilst the vortex line of most intense vorticity remains more or less parallel to the (x, y) plane. Further, a progressive inward displacement of the vorticity core is noticeable, due to the attraction of the similar vortex system at the other tip.*

Vortex Strength deduced from Measurements of Circulation.

11. The vorticity diagrams discussed in §10 show that a large part of the flow in the aërofoil wake is irrotational and that the vorticity is confined to a relatively small volume. To illustrate this point, values of $\int(vdy + wdz)$ were calculated around the contours of two series of rectangles contained between lines parallel to the axes of y and z. The first series of rectangles were bounded by two horizontal lines (z = const.), suitably spaced so as just to contain the vortex region; these rectangles were of increasing width, with the vertical line of symmetry ($y = 3$) as a common side. In the second series, the horizontal lines were much further apart, and were taken close to the upper and lower boundaries of the field, the vertical boundaries being the same as before. The results of these calculations are given in Table II.

TABLE II.—Values of the Circulation, $\int(vdy + wdz)$, Measured around Rectangular Contours formed by the Lines $z = z_1$, $z = z_2$, $y = 3$, and $y = y$.

y	Section B (x -0.573)		Section C ($x = -2$)		Section D ($x = -13$)	
	$z_1 = -0.238$ $z_2 = 0.187$	$z_1 = -0.388$ $z_2 = 0.313$	$z_1 = -0.350$ $z_2 = 0.297$	$z_1 = -0.530$ $z_2 = 0.573$	$z_1 = -0.350$ $z_2 = 0.278$	$z_1 = -0.577$ $z_2 = 0.483$
3.0	0	0	0	0	0	0
2.0	0.011	0.012	0.014	0.011	0.005	0
1.0	0.054	0.062	0.060	0.058	0.013	0.004
0.5	0.112	0.119	0.111	0.108	0.030	0.022
0.4	0.128	0.135	0.124	0.120	0.043	0.036
0.3	0.147	0.151	0.137	0.134	0.087	0.096
0.2	0.169	0.170	0.155	0.152	0.240	0.270
0.15	0.184	0.183	0.196	0.190	0.280	0.290
0.1	0.205	0.215	0.295	0.276	0.297	0.302
0.05	0.290	0.304	0.378	0.374	0.305	0.314
0	0.392	0.390	0.405	0.392	0.310	0.323
−0.1	0.406	0.409	0.415	0.409	0.320	0.337
−0.5	0.414	0.414	0.420	0.416	0.331	0.342
−1.5	0.414	0.414	0.420	0.416	0.331	0.342

* Cf. LAMB, 'Hydrodynamics,' §155.

Close agreement is observed between the two sets of results for Sections B and C, and also, to a lesser extent, for Section D, and this shows that the flow above and below each inner pair of horizontal lines is irrotational. The results also shows that the flow beyond the aërofoil tip is irrotational. Further, since the circulation around a closed contour is equal to the total strength of the vorticity within the contour, it follows that the values in the table represent the total strength of the vorticity within vertical strips of increasing width, the line of symmetry ($y = 3$) being a common side.

12. Comparisons will now be made between these measured vortex strengths and the values immediately behind the trailing edge, as estimated theoretically from the distribution of lift along the aërofoil. According to the PRANDTL theory,* the strength of the vorticity leaving an element of the aërofoil is equal to the change, along the length, of the circulation around the element; thus, if K_a be the circulation at any section $\left(\frac{\partial K_a}{\partial y}\right) \cdot dy$ is the strength of the longitudinal vortex leaving the element of length dy, and this becomes $\left(\frac{\partial K_L}{\partial y}\right)dy$ V . C by virtue of the relation† $K_a = K_L . V . C.$, where K_L is the lift coefficient, C the chord, and V the velocity of the undisturbed air. Hence when V and C are each taken as unity, and the total vortex strength κ is measured from the line of symmetry ($y = 3$), it follows that the value of κ at the point y is given by

$$\int_y^{y=3} \left(\frac{\partial K_a}{\partial y}\right) dy = \int_y^{y=3} \left(\frac{\partial K_L}{\partial y}\right) dy = [(K_L)_{y=3} - (K_L)_y].$$

Theoretically, then, the total vortex strength in a field taken immediately behind the aërofoil, and extending from the plane of symmetry outwards, is equal to the circulation around the median section; and also, that the distribution of vortex strength is directly related to the distribution of lift on the aërofoil.

13. Values of the total vortex strength in the Sections B, C, and D, as measured from the line of symmetry outwards, are compared in Table III with those of the circulation taken around the median section of the aërofoil.

TABLE III.

(Circulation) Lift coefficient, K_L at medium section.		Total vortex strength in the entire field extending from the line of symmetry outwards.		
From Pressure Measurements.	From PRANDTL Theory.	Section B $x = -0.573$	Section C $x = -2$	Section D $x = -13$
0·415	0·420	0·414	0·416	0·342

* An outline of this theory, and also references, is given in a paper by L. PRANDTL. "Application of Modern Hydrodynamics to Aëronautics." 'Report No. 116, American Advisory Committee for Aëronautics.'

† This relation is deduced from the KUTTA-JOUKOWSKY's law, which states that the lift per unit length of an aërofoil placed in a stream of perfect fluid is equal to the product $K_a \rho V$. This relation has been experimentally verified by BRYANT and WILLIAMS for an infinite aërofoil in a current of air (loc. cit.).

With the exception of Section D (13 chords behind), the two sets of results are in very close agreement, and the comparison shows that the measured total strength of the vorticity is equal to the circulation around the median section. Attention is directed to the difference, amounting to about 18 per cent. of the total vorticity, between the value at Section D and those at Sections B and C; it is thought that a part of this difference may be due to a dissipation of vorticity and that the remainder has been transferred to a region outside that explored.

14. In fig. 9 the experimental values of κ given in Table II are plotted against y, together with the values of $[(K_L)_{y=3} - (K_L)_y]$ estimated from the theoretical and
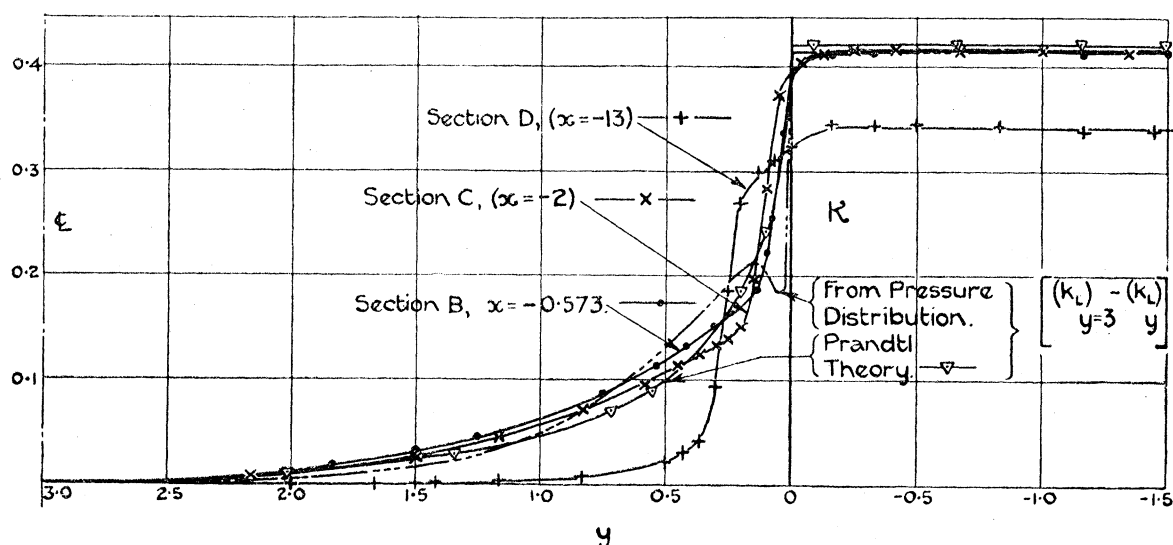
Fɪɢ. 9.—Curves of Total Vortex Strength, κ, measured between the line of Symmetry $(y = 3)$ and lines $y = $ constant.

experimental values of K_L given in Table I. It is seen that the distribution of vorticity in Section B $(x = -0.573)$, and to a lesser extent in Section C $(x = -2)$, closely resembles that estimated from the theoretical lift curve. The curves also illustrate the changes in the distribution of vorticity along the span, and the marked accumulation in the neighbourhood of the tip.

15. The distribution of vortex strength across each section is given in fig. 10, where values of $(\partial \kappa / \partial y)$ are plotted against y. The full lines in these diagrams have been drawn through values obtained directly from the measured slopes of the (κ, y) curves of fig. 9, whilst the points represent the values obtained from integration along z ordinates of the vorticity values given in fig. 8. The two sets of results are seen to be in close agreement, an indication that in both cases the accuracy of measurement is satisfactory.

The diagrams clearly show the concentration of the vortex strength within a small region behind the aërofoil tip, also the marked inward traverse of the tip vortex, which accompanies its motion down-stream.
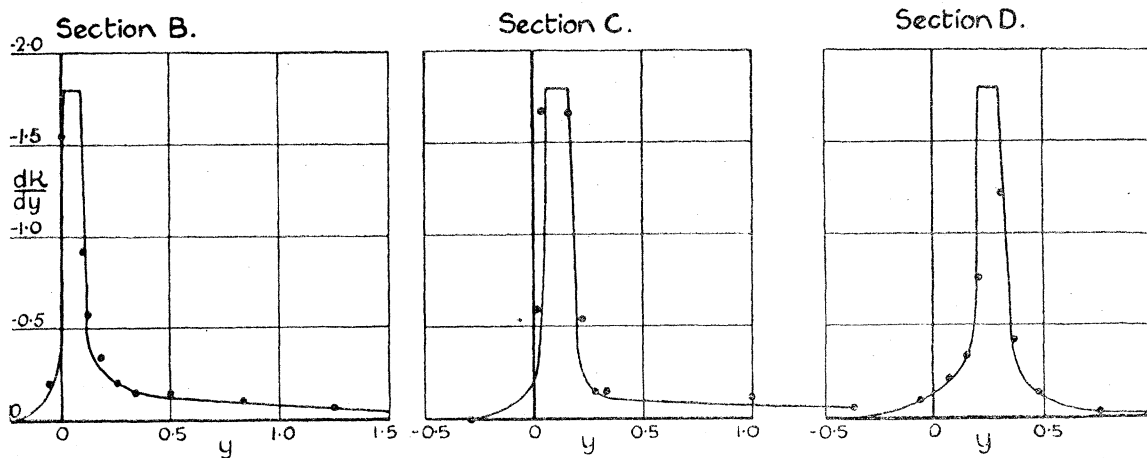
FIG. 10.—Values of $\frac{d\kappa}{dy}$. Full Lines obtained from the slopes of curves in Fig. 9. Points are the values of $\int\left(\frac{\partial w}{\partial y} - \frac{\partial v}{\partial z}\right) dz$ from Fig. 8.

16. Calculations of the circulation in the (y, z) plane at Section A (forward of the aërofoil) led to an important result. Two sets of rectangles were taken, the first contained between the horizontal lines $(z = 0\cdot42)$ and $(z = -0\cdot61)$, and the second between the lines $(z = -0\cdot01)$ and $(z = -0\cdot185)$; the width of each rectangle was $0\cdot5$ chord. The results of these calculations are given in Table IV.

TABLE IV.—Values of the Circulation Measured around Rectangular Contours formed by the Lines $z = z_1$, $z = z_2$, $y = y_1$, $y = y_2$.

y_1	y_2	First Set. $z_1 = 0\cdot42$ $z_2 = -0\cdot61$	Second Set. $z_1 = -0\cdot01$ $z_2 = -0\cdot185$
$3\cdot0$	$2\cdot5$	0	$0\cdot0015$
$2\cdot5$	$2\cdot0$	$0\cdot0002$	$0\cdot0011$
$2\cdot0$	$1\cdot5$	$0\cdot0008$	$0\cdot0004$
$1\cdot5$	$1\cdot0$	$0\cdot0015$	0
$1\cdot0$	$0\cdot5$	$0\cdot0015$	$-0\cdot0006$
$0\cdot5$	0	$-0\cdot0019$	$-0\cdot0012$
0	$-0\cdot5$	$+0\cdot0013$	$+0\cdot0013$
$-0\cdot5$	$-1\cdot0$	$-0\cdot0024$	$+0\cdot0005$
$-1\cdot0$	$-1\cdot5$	$-0\cdot0049$	$-0\cdot0003$

The possible inaccuracy in the measurements of v and w is about $\pm 0\cdot0025$, so that the circulations are uncertain to within about $\pm 0\cdot0050$ (first set) and $\pm 0\cdot0030$ (second set); it thus appears, from the values given in the table, that the circulation in front of the aërofoil is zero, within the limits of experimental accuracy.

Continuity.

17. The general equation of continuity—that is,

$$\frac{\partial u}{\partial x} + \frac{\partial v}{\partial y} + \frac{\partial w}{\partial z} = 0,$$

reduces to

$$\frac{\partial v}{\partial y} + \frac{\partial w}{\partial z} = 0,$$

if u is independent of y and z, so that relative to this longitudinal velocity, the flow in each (y, z) plane is two-dimensional and a stream function ψ can be considered to exist.

There was good reason to believe, since the variations of u behind the aërofoil were small, that the equation $\left(\frac{\partial v}{\partial y} + \frac{\partial w}{\partial z}\right) = 0$ would be satisfied in each of the (y, z) planes of exploration. Accordingly, the following calculations have been made, the purpose being first to show that this equation was satisfied within the limits of experimental accuracy, and then to represent the flow pattern, in the conventional manner, by diagrams of ψ.

This equation is satisfied if the flow across every line that can be drawn between any two points in the field is the same. The method of examination adopted was to draw lines parallel to the axes of y and z, so that several alternative paths connected any two points A and B in the field. The flow across each of these paths was then evaluated by substituting the experimental values of v and w in the expansion integral $\int_{B}^{A}(w\,dy - v\,dz)$.

In every case one of the points was taken in the line $y = 3$, which was assumed from considerations of symmetry to be a stream-line, ψ_0.

18. To illustrate the method, the procedure followed for Section C will be described in outline. Twenty-four datum points, well distributed in the field, were obtained from the intersection of the lines

$$y = \quad 1 \cdot 667, \quad 0 \cdot 667, \; - \; 0 \cdot 333, \; - \; 0 \cdot 833, \text{ and}$$
$$z = - \; 1 \cdot 083, \; - \; 0 \cdot 667, \; - \; 0 \cdot 333, \quad 0 \cdot 25, \; 0 \cdot 583, \text{ and } 0 \cdot 917.$$

The quantity of fluid flowing between each of these points and the stream-line ψ_0 was then determined for the six different paths given by the horizontal lines ($z = $ constant) and the particular vertical line passing through the point.

Representative results are given in Table V, where the six values of $(\psi_0 - \psi)$ for each of the datum points on the lines $y = 0 \cdot 667$ and $(y = -0 \cdot 333)$ are compared. The values in any one group are in close agreement, and do not appear to follow any systematic variation. In the last column (ξ) of Table V are given the velocity values obtained when the differences between the mean and measured values of $(\psi_0 - \psi)$

are divided by the appropriate length of path.   These differences are seen to be small, and in all cases are less than the probable errors of observation ($\pm 0 \cdot 0025$).   It thus appears that the condition for continuity is satisfied in Section C, within the limits of experimental error.

TABLE V.—A path starts from the line of symmetry ($y = 3$), traverses a line $z = a$ and then a line $y = b$ to the datum point. ξ = difference between the mean and measured values of ($\psi_0 - \psi$) divided by the length of the path.

Datum point.	Path		($\psi_0 - \psi$).	Mean value of ($\psi_0 - \psi$).	ξ.
	a.	b.			
$y = \quad 0 \cdot 667$ $z = -1 \cdot 083$	$-1 \cdot 083$	$0 \cdot 667$	$0 \cdot 0956$		$-0 \cdot 0003$
	$-0 \cdot 667$	$0 \cdot 667$	$0 \cdot 0971$		$-0 \cdot 0008$
	$-0 \cdot 333$	$0 \cdot 667$	$0 \cdot 0939$	$0 \cdot 0948$	$+0 \cdot 0003$
	$0 \cdot 250$	$0 \cdot 667$	$0 \cdot 0923$		$+0 \cdot 0007$
	$0 \cdot 583$	$0 \cdot 667$	$0 \cdot 0975$		$-0 \cdot 0007$
	$0 \cdot 917$	$0 \cdot 667$	$0 \cdot 0922$		$+0 \cdot 0006$
$y = \quad 0 \cdot 667$ $z = -0 \cdot 667$	$-1 \cdot 083$	$0 \cdot 667$	$0 \cdot 1171$		$-0 \cdot 0003$
	$-0 \cdot 667$	$0 \cdot 667$	$0 \cdot 1186$		$-0 \cdot 0010$
	$-0 \cdot 333$	$0 \cdot 667$	$0 \cdot 1154$	$0 \cdot 1163$	$+0 \cdot 0003$
	$0 \cdot 250$	$0 \cdot 667$	$0 \cdot 1138$		$+0 \cdot 0008$
	$0 \cdot 583$	$0 \cdot 667$	$0 \cdot 1190$		$-0 \cdot 0007$
	$0 \cdot 917$	$0 \cdot 667$	$0 \cdot 1137$		$+0 \cdot 0007$
$y = \quad 0 \cdot 667$ $z = -0 \cdot 333$	$-1 \cdot 083$	$0 \cdot 667$	$0 \cdot 1365$		$-0 \cdot 0003$
	$-0 \cdot 667$	$0 \cdot 667$	$0 \cdot 1380$		$-0 \cdot 0009$
	$-0 \cdot 333$	$0 \cdot 667$	$0 \cdot 1348$	$0 \cdot 1357$	$+0 \cdot 0004$
	$0 \cdot 250$	$0 \cdot 667$	$0 \cdot 1332$		$+0 \cdot 0009$
	$0 \cdot 583$	$0 \cdot 667$	$0 \cdot 1384$		$-0 \cdot 0008$
	$0 \cdot 917$	$0 \cdot 667$	$0 \cdot 1331$		$+0 \cdot 0007$
$y = \quad 0 \cdot 667$ $z = \quad 0 \cdot 250$	$-1 \cdot 083$	$0 \cdot 667$	$0 \cdot 1465$		$-0 \cdot 0002$
	$-0 \cdot 667$	$0 \cdot 667$	$0 \cdot 1480$		$-0 \cdot 0008$
	$-0 \cdot 333$	$0 \cdot 667$	$0 \cdot 1448$	$0 \cdot 1457$	$+0 \cdot 0003$
	$0 \cdot 250$	$0 \cdot 667$	$0 \cdot 1432$		$+0 \cdot 0011$
	$0 \cdot 583$	$0 \cdot 667$	$0 \cdot 1484$		$-0 \cdot 0010$
	$0 \cdot 917$	$0 \cdot 667$	$0 \cdot 1431$		$+0 \cdot 0009$
$y = \quad 0 \cdot 667$ $z = \quad 0 \cdot 583$	$-1 \cdot 083$	$0 \cdot 667$	$0 \cdot 1221$		$-0 \cdot 0002$
	$-0 \cdot 667$	$0 \cdot 667$	$0 \cdot 1236$		$-0 \cdot 0006$
	$-0 \cdot 333$	$0 \cdot 667$	$0 \cdot 1204$	$0 \cdot 1213$	$+0 \cdot 0003$
	$0 \cdot 250$	$0 \cdot 667$	$0 \cdot 1188$		$+0 \cdot 0009$
	$0 \cdot 583$	$0 \cdot 667$	$0 \cdot 1240$		$-0 \cdot 0012$
	$0 \cdot 917$	$0 \cdot 667$	$0 \cdot 1187$		$+0 \cdot 0010$
$y = \quad 0 \cdot 667$ $z = \quad 0 \cdot 917$	$-1 \cdot 083$	$0 \cdot 667$	$0 \cdot 1033$		$-0 \cdot 0002$
	$-0 \cdot 667$	$0 \cdot 667$	$0 \cdot 1048$		$-0 \cdot 0006$
	$-0 \cdot 333$	$0 \cdot 667$	$0 \cdot 1016$	$0 \cdot 1025$	$+0 \cdot 0002$
	$0 \cdot 250$	$0 \cdot 667$	$0 \cdot 1000$		$+0 \cdot 0008$
	$0 \cdot 583$	$0 \cdot 667$	$0 \cdot 1052$		$-0 \cdot 0010$
	$0 \cdot 917$	$0 \cdot 667$	$0 \cdot 0999$		$+0 \cdot 0011$

TABLE V—*continued*.

Datum point.	Path		$(\psi_0 - \psi)$.	Mean value of $(\psi_0 - \psi)$.	ξ.
	a.	b.			
$y = -0.333$ $z = -1.083$	−1.083	−0.333	0.1002		−0.0020
	−0.667	−0.333	0.0996		−0.0016
	−0.333	−0.333	0.0918		+0.0004
	+0.250	−0.333	0.0875	0.0934	+0.0013
	0.583	−0.333	0.0948		−0.0003
	0.917	−0.333	0.0867		+0.0013
$y = -0.333$ $z = -0.667$	−1.083	−0.333	0.1236		−0.0018
	−0.667	−0.333	0.1231		−0.0018
	−0.333	−0.333	0.1154		+0.0004
	0.250	−0.333	0.1111	0.1170	−0.0014
	0.583	−0.333	0.1184		−0.0003
	0.917	−0.333	0.1103		+0.0014
$y = -0.333$ $z = -0.333$	−1.083	−0.333	0.1433		−0.0017
	−0.667	−0.333	0.1426		−0.0017
	−0.333	−0.333	0.1349		+0.0005
	0.250	−0.333	0.1306	0.1365	+0.0015
	0.583	−0.333	0.1379		−0.0003
	0.917	−0.333	0.1298		+0.0015
$y = -0.333$ $z = 0.250$	−1.083	−0.333	0.1419		−0.0015
	−0.667	−0.333	0.1412		−0.0014
	−0.333	−0.333	0.1335		+0.0004
	0.250	−0.333	0.1292	0.1351	+0.0018
	0.583	−0.333	0.1365		−0.0004
	0.917	−0.333	0.1284		+0.0017
$y = -0.333$ $z = 0.583$	−1.083	−0.333	0.1249		−0.0014
	−0.667	−0.333	0.1242		−0.0013
	−0.333	−0.333	0.1165		+0.0004
	0.250	−0.333	0.1122	0.1181	+0.0016
	0.583	−0.333	0.1195		−0.0004
	0.917	−0.333	0.1114		+0.0018
$y = -0.333$ $z = 0.917$	−1.083	−0.333	0.1091		−0.0013
	−0.667	−0.333	0.1084		−0.0012
	−0.333	−0.333	0.1007		+0.0004
	0.250	−0.333	0.0964	0.1023	+0.0015
	0.583	−0.333	0.1037		−0.0004
	0.917	−0.333	0.0956		+0.0020

19. Continuity of flow was established for the Sections B and D in a similar manner. The agreement between the measured and mean values of $(\psi_0 - \psi)$ was not as satisfactory as for Section C, but even in the worst cases the velocity differences, given by the ratio of $(\psi_0 - \psi)$ to the length of the path, did not exceed the limit ± 0.005.

The equation for continuity of flow in the (y, z) plane forward of the aerofoil (Section A)

was not satisfied, a result to be expected in view of the longitudinal acceleration of air, due to the presence of the aërofoil.

"ψ" Diagrams.

20. Since it has been shown that the continuity equation $\left(\dfrac{\partial v}{\partial y} + \dfrac{\partial w}{\partial z}\right)$ is satisfied over the Sections B, C, and D, there must exist at each point in these (y, z) planes a function ψ, such that

$$v = -\frac{\partial \psi}{\partial z} \text{ and } w = \frac{\partial \psi}{\partial y}.$$

The values of ψ were determined by the method of § 18 ; they represent the mean values obtained from the flow measured across six different paths connecting the point in question to the symmetrical stream-line $y = 3$; for convenience, the zero was taken at the centre of the vortex system.

Diagrams showing, for each section, contour lines of equal value of ψ are given in figs. 11–13. For the interpretation of these diagrams it is necessary to consider the
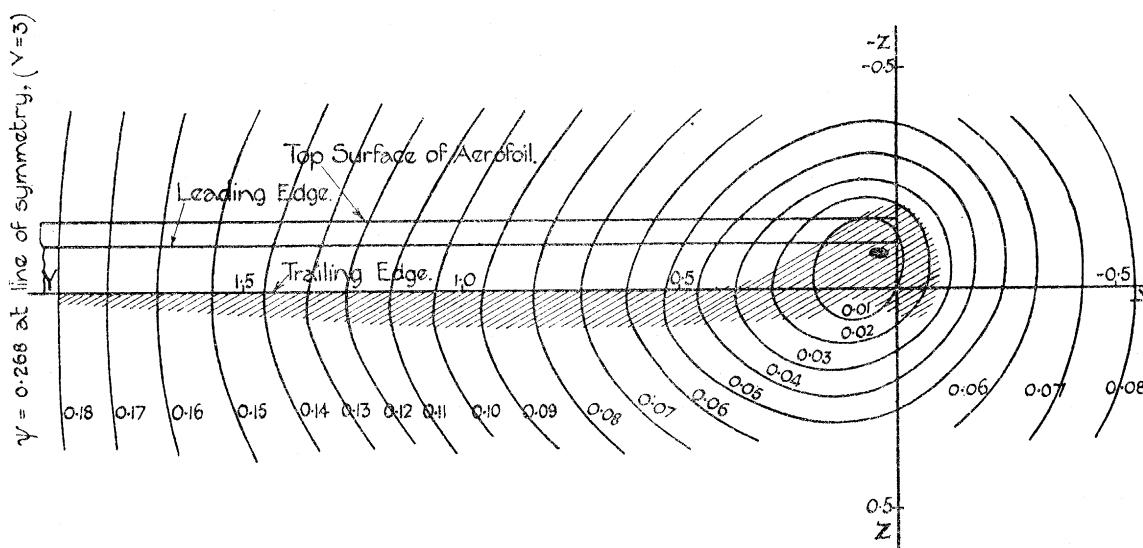
Fig. 11.—Section B (0·57 chord behind).

physical significance of the quantity ψ. According to the definition of § 17, the difference between the values of ψ at any two points represents the flow across any line joining the points ; it is therefore analogous to the stream-line function of two-dimensional flow, so that if the flow remained unchanged down-stream of the aërofoil, the contours of equal ψ would be the actual stream-lines as seen by an observer moving with the stream. Actually, slight changes occur in the flow pattern, so that these conditions are only approximately true.

The diagrams illustrate clearly the changes in the character of the airflow behind the aërofoil : close to the aërofoil, the contour lines are ovals with the ends pointing inwards ;
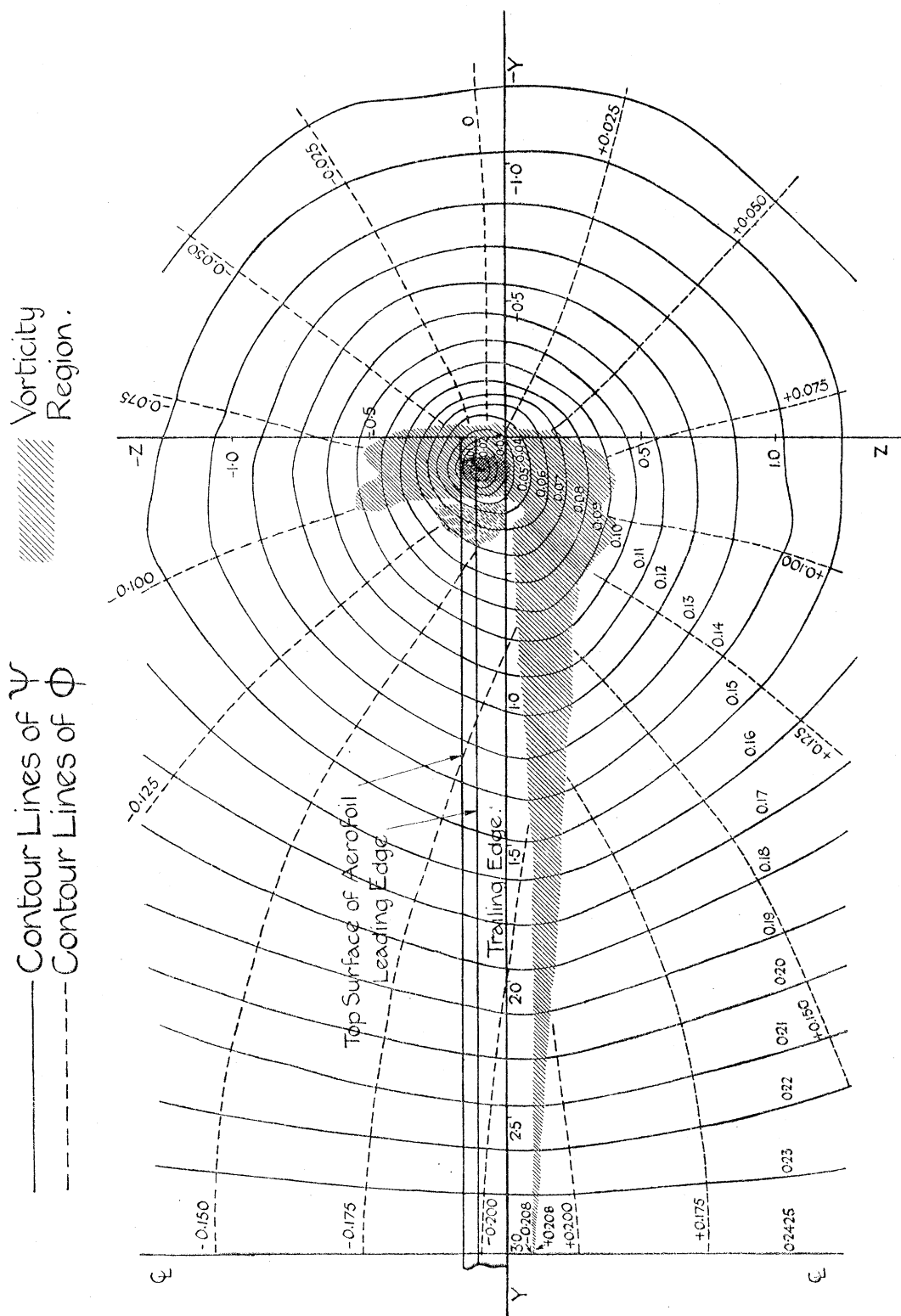
Fig. 12.—Section C (two chords behind).

2 U 2
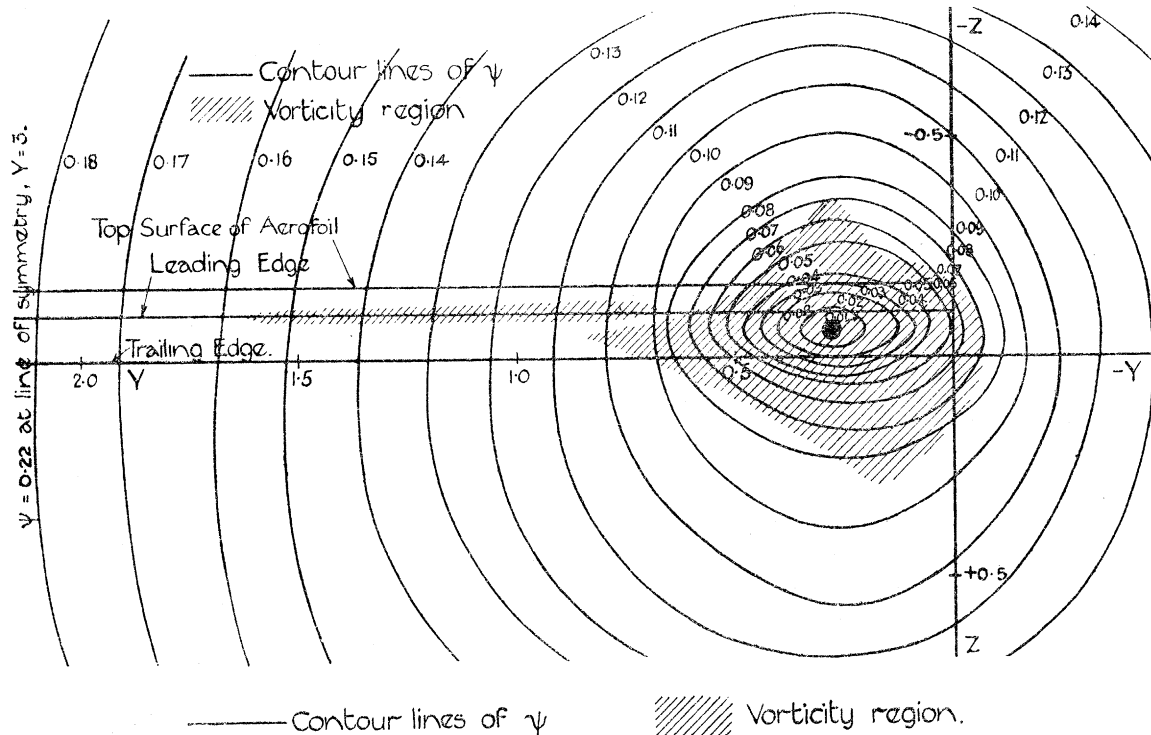
Fɪɢ. 13.—Section D (13 chords behind).

as the distance behind the aërofoil increases, the contour lines become more and more circular—indicating that the vorticity is becoming more concentrated.

Velocity Potential φ.

21. Contour lines of equal value of φ are given, for the irrotational region of Section C, in fig. 12. The values of φ along the symmetrical line, $y = 3$, were determined directly from $\int w\,dz$ taken along this line ($v = 0$), but elsewhere the values are the means determined from the measured circulation $\int (v\,dy + w\,dz)$ along six different paths taken in the irrotational region. In this way, a contour line was obtained outside the aërofoil tip which was almost parallel to the trailing edge, and this line was taken as $\phi = 0$.

The chief interest in the "φ" lines given in fig. 12 is that they illustrate the cyclic character of the function φ. It will be noticed from a comparison with Table III that the difference in the two values of φ on opposite sides of the vortex sheet at $y = 3$ is equal to the total vortex strength leaving a semi-span of the aërofoil.

22. In conclusion, the authors wish to acknowledge their great indebtedness to Prof. L. Bairstow, F.R.S., and Dr. H. Lamb, F.R.S., for valuable criticisms and suggestions; to Mr. H. E. Falkner, an advanced student from the Imperial College of Science and Technology, for valuable service given during the experimental stage of the work; and to Mr. T. A. Kirkup for general assistance given in the reduction of the results.

TABLE VI.—Section A ($1 \cdot 51$ chords in front of trailing edge of aërofoil).   Experimental Results.   (Hot-wire.)

y Chords.	$z = -0 \cdot 613$			$z = -0 \cdot 342$			$z = -0 \cdot 185$		
	$-u$	v	w	u	v	w	$-u$	v	w
$3 \cdot 000$	$1 \cdot 037$	$-0 \cdot 005$	$-0 \cdot 054$	$1 \cdot 031$	0	$-0 \cdot 068$	$0 \cdot 998$	$-0 \cdot 003$	$-0 \cdot 067$
$2 \cdot 333$	$1 \cdot 037$	$-0 \cdot 010$	$-0 \cdot 054$	$1 \cdot 031$	$-0 \cdot 003$	$-0 \cdot 068$	$0 \cdot 998$	$-0 \cdot 004$	$-0 \cdot 064$
$1 \cdot 667$	$1 \cdot 037$	$-0 \cdot 011$	$-0 \cdot 054$	$1 \cdot 031$	$-0 \cdot 003$	$-0 \cdot 065$	$0 \cdot 990$	$-0 \cdot 005$	$-0 \cdot 059$
$1 \cdot 000$	$1 \cdot 037$	$-0 \cdot 010$	$-0 \cdot 053$	$1 \cdot 031$	$-0 \cdot 003$	$-0 \cdot 058$	$0 \cdot 986$	$-0 \cdot 006$	$-0 \cdot 054$
$0 \cdot 500$	$1 \cdot 033$	$-0 \cdot 007$	$-0 \cdot 050$	$1 \cdot 031$	$-0 \cdot 003$	$-0 \cdot 051$	$0 \cdot 986$	$-0 \cdot 009$	$-0 \cdot 048$
$0 \cdot 333$	$1 \cdot 030$	$-0 \cdot 005$	$-0 \cdot 047$	$1 \cdot 031$	$-0 \cdot 003$	$-0 \cdot 048$	$0 \cdot 988$	$-0 \cdot 010$	$-0 \cdot 045$
$0 \cdot 167$	$1 \cdot 021$	$-0 \cdot 003$	$-0 \cdot 043$	$1 \cdot 030$	$-0 \cdot 002$	$-0 \cdot 043$	$0 \cdot 995$	$-0 \cdot 010$	$-0 \cdot 042$
0	$1 \cdot 018$	$-0 \cdot 004$	$-0 \cdot 040$	$1 \cdot 011$	$-0 \cdot 001$	$-0 \cdot 037$	$0 \cdot 998$	$-0 \cdot 011$	$-0 \cdot 039$
$-0 \cdot 167$	$1 \cdot 025$	$-0 \cdot 008$	$-0 \cdot 037$	$1 \cdot 000$	$+0 \cdot 001$	$-0 \cdot 034$	$0 \cdot 999$	$-0 \cdot 009$	$-0 \cdot 036$
$-0 \cdot 333$	$1 \cdot 027$	$-0 \cdot 008$	$-0 \cdot 034$	$1 \cdot 003$	$0 \cdot 002$	$-0 \cdot 033$	$1 \cdot 000$	$-0 \cdot 006$	$-0 \cdot 034$
$-0 \cdot 500$	$1 \cdot 028$	$-0 \cdot 007$	$-0 \cdot 032$	$1 \cdot 010$	$0 \cdot 002$	$-0 \cdot 032$	$1 \cdot 000$	$-0 \cdot 004$	$-0 \cdot 031$
$-1 \cdot 000$	$1 \cdot 030$	$-0 \cdot 004$	$-0 \cdot 031$	$1 \cdot 012$	$0 \cdot 003$	$-0 \cdot 027$	$1 \cdot 004$	$+0 \cdot 001$	$-0 \cdot 022$
$-1 \cdot 500$	$1 \cdot 030$	$-0 \cdot 001$	$-0 \cdot 030$	$1 \cdot 012$	$0 \cdot 003$	$-0 \cdot 023$	$1 \cdot 004$	$0 \cdot 003$	$-0 \cdot 012$

y Chords.	$z = -0 \cdot 01$			$z = +0 \cdot 142$			$z = +0 \cdot 417$		
	$-u$	v	w	$-u$	v	w	$-u$	v	w
$3 \cdot 000$	$0 \cdot 984$	$-0 \cdot 006$	$-0 \cdot 048$	$0 \cdot 964$	0	$-0 \cdot 041$	$0 \cdot 962$	$-0 \cdot 006$	$-0 \cdot 029$
$2 \cdot 333$	$0 \cdot 984$	$-0 \cdot 006$	$-0 \cdot 048$	$0 \cdot 964$	$-0 \cdot 003$	$-0 \cdot 038$	$0 \cdot 964$	$-0 \cdot 013$	$-0 \cdot 029$
$1 \cdot 667$	$0 \cdot 984$	$-0 \cdot 006$	$-0 \cdot 048$	$0 \cdot 964$	$-0 \cdot 005$	$-0 \cdot 035$	$0 \cdot 974$	$-0 \cdot 016$	$-0 \cdot 029$
$1 \cdot 000$	$0 \cdot 984$	$-0 \cdot 006$	$-0 \cdot 048$	$0 \cdot 968$	$-0 \cdot 007$	$-0 \cdot 033$	$0 \cdot 974$	$-0 \cdot 018$	$-0 \cdot 029$
$0 \cdot 500$	$0 \cdot 984$	$-0 \cdot 009$	$-0 \cdot 047$	$0 \cdot 970$	$-0 \cdot 010$	$-0 \cdot 031$	$0 \cdot 978$	$-0 \cdot 019$	$-0 \cdot 030$
$0 \cdot 333$	$0 \cdot 984$	$-0 \cdot 010$	$-0 \cdot 041$	$0 \cdot 972$	$-0 \cdot 011$	$-0 \cdot 030$	$0 \cdot 978$	$-0 \cdot 019$	$-0 \cdot 030$
$0 \cdot 167$	$0 \cdot 984$	$-0 \cdot 012$	$-0 \cdot 034$	$0 \cdot 972$	$-0 \cdot 011$	$-0 \cdot 030$	$0 \cdot 976$	$-0 \cdot 019$	$-0 \cdot 030$
0	$0 \cdot 988$	$-0 \cdot 014$	$-0 \cdot 033$	$0 \cdot 975$	$-0 \cdot 012$	$-0 \cdot 030$	$0 \cdot 978$	$-0 \cdot 019$	$-0 \cdot 030$
$-0 \cdot 167$	$0 \cdot 988$	$-0 \cdot 014$	$-0 \cdot 033$	$0 \cdot 980$	$-0 \cdot 012$	$-0 \cdot 030$	$0 \cdot 985$	$-0 \cdot 019$	$-0 \cdot 030$
$-0 \cdot 333$	$0 \cdot 984$	$-0 \cdot 012$	$-0 \cdot 032$	$0 \cdot 991$	$-0 \cdot 011$	$-0 \cdot 030$	$1 \cdot 002$	$-0 \cdot 019$	$-0 \cdot 030$
$-0 \cdot 500$	$0 \cdot 984$	$-0 \cdot 008$	$-0 \cdot 031$	$1 \cdot 004$	$-0 \cdot 011$	$-0 \cdot 029$	$1 \cdot 005$	$-0 \cdot 017$	$-0 \cdot 030$
$-1 \cdot 000$	$0 \cdot 990$	$-0 \cdot 002$	$-0 \cdot 022$	$1 \cdot 004$	$-0 \cdot 001$	$-0 \cdot 024$	$1 \cdot 006$	$-0 \cdot 006$	$-0 \cdot 029$
$-1 \cdot 500$	$0 \cdot 994$	0	$-0 \cdot 015$	$1 \cdot 004$	$+0 \cdot 004$	$-0 \cdot 020$	$1 \cdot 006$	$-0 \cdot 001$	$-0 \cdot 024$

TABLE VII.—Section B (0·573 chord behind trailing edge of aërofoil).   Experimental Results.   (Hot-wire.)

y Chords.	$z = +0\cdot313$			$z = +0\cdot187$			$z = +0\cdot068$		
	$-u$	v	w	$-u$	v	w	$-u$	v	w
2·833	0·998	—0·003	0·074	0·998	—0·002	0·075	0·996	—0·011	0·080
2·167	0·998	—0·008	0·079	0·998	—0·010	0·083	0·996	—0·021	0·084
1·667	0·998	—0·017	0·081	1·000	—0·015	0·086	0·996	—0·030	0·087
1·333	0·998	—0·027	0·081	1·000	—0·025	0·086	0·996	—0·035	0·089
1·000	0·998	—0·042	0·079	1·000	—0·044	0·087	0·996	—0·041	0·092
0·833	0·998	—0·052	0·076	1·000	—0·057	0·087	0·996	—0·048	0·092
0·667	0·998	—0·064	0·072	1·000	—0·074	0·084	0·996	—0·060	0·093
0·500	0·998	—0·081	0·064	1·000	—0·094	0·080	0·996	—0·082	0·094
0·417	0·998	—0·090	0·057	1·000	—0·106	0·075	0·996	—0·097	0·095
0·353	1·007	—0·100	0·047	1·007	—0·122	0·067	1·015	—0·121	0·094
0·250	1·013	—0·108	0·032	1·012	—0·142	0·050	1·040	—0·161	0·089
0·183	1·012	—0·112	+0·015	1·020	—0·157	+0·024	1·050	—0·195	0·072
0·117	1·010	—0·113	0	1·027	—0·171	—0·006	1·054	—0·230	+0·010
0·067	1·010	—0·111	—0·013	1·031	—0·172	—0·032	1·054	—0·263	—0·047
0·017	1·010	—0·104	—0·025	1·033	—0·161	—0·059	1·048	—0·240	—0·116
—0·067	1·010	—0·092	—0·045	1·027	—0·132	—0·084	1·043	—0·164	—0·164
—0·167	1·021	—0·076	—0·056	1·015	—0·090	—0·089	1·030	—0·079	—0·151
—0·333	1·021	—0·050	—0·058	1·015	—0·045	—0·083	1·010	—0·027	—0·109
—0·500	1·021	—0·030	—0·055	1·015	—0·026	—0·071	1·010	—0·010	—0·079
—0·833	1·021	—0·010	—0·041	1·015	—0·009	—0·049	1·010	+0·001	—0·051
—1·167	1·021	—0·002	—0·030	1·015	—0·003	—0·036	1·010	+0·005	—0·037
—1·500	1·021	0	—0·026	1·015	0	—0·031	1·010	+0·006	—0·032

y Chords.	$z = 0$			$z = -0\cdot055$			$z = -0\cdot072$		
	$-u$	v	w	$-u$	v	w	$-u$	v	w
2·833	1·000	0	0·095	0·980	0·004	0·082	0·986	0·004	0·087
2·167	1·000	0·002	0·096	0·980	0·012	0·085	0·986	0·012	0·090
1·667	1·000	0·010	0·099	0·980	0·017	0·087	0·986	0·021	0·092
1·333	1·000	0·016	0·100	0·980	0·026	0·089	0·986	0·029	0·094
1·000	1·000	0·028	0·104	0·980	0·041	0·094	0·986	0·041	0·096
0·833	1·000	0·037	0·107	0·980	0·052	0·098	0·986	0·050	0·098
0·667	1·000	0·047	0·112	0·980	0·062	0·102	0·986	0·060	0·102
0·500	1·007	0·055	0·119	0·980	0·070	0·110	0·986	0·069	0·109
0·417	1·011	0·054	0·123	0·980	0·069	0·116	0·986	0·074	0·119
0·333	1·017	0·042	0·128	0·990	0·065	0·130	0·986	0·078	0·137
0·250	1·027	+0·014	0·132	1·000	0·051	0·179	0·986	0·075	0·169
0·183	1·040	—0·046	0·131	1·022	+0·003	0·244	1·010	+0·057	0·245
0·117	1·065	—0·220	+0·113	1·032	—0·225	0·345	1·070	—0·070	0·435
0·067	1·084	—0·310	—0·002	1·015	—0·420	+0·100	1·085	—0·190	+0·150
0·017	1·080	—0·320	—0·160	1·005	—0·350	—0·430	0·970	+0·010	—0·470
—0·067	1·015	—0·146	—0·239	1·030	—0·054	—0·318	1·004	0·016	—0·345
—0·167	1·010	—0·049	—0·179	1·007	—0·004	—0·202	1·004	0·006	—0·200
—0·333	1·010	—0·009	—0·112	0·996	+0·004	—0·104	1·007	0·006	—0·115
—0·500	1·010	—0·003	—0·084	0·996	0·004	—0·079	1·000	0·006	—0·083
—0·833	1·010	0	—0·056	0·996	0·004	—0·051	1·000	0·006	—0·046
—1·167	1·010	+0·004	—0·039	0·996	0·004	—0·035	1·000	0·006	—0·033
—1·500	1·010	+0·007	—0·028	0·996	0·004	—0·028	1·000	0·006	—0·026

TABLE VII—*continued*.

y Chords.	$z = -0.088$			$z = -0.179$		
	$-u$	v	w	$-u$	v	w
2·833	0·986	0·006	0·082	1·008	0·008	0·089
2·167	0·986	0·014	0·085	1·008	0·015	0·089
1·667	0·986	0·020	0·087	1·008	0·020	0·090
1·333	0·986	0·028	0·088	1·008	0·028	0·090
1·000	0·986	0·040	0·092	1·014	0·039	0·090
0·833	0·990	0·049	0·096	1·017	0·047	0·091
0·667	0·990	0·058	0·099	1·020	0·059	0·094
0·500	0·990	0·070	0·105	1·020	0·073	0·099
0·417	0·987	0·077	0·111	1·020	0·083	0·106
0·333	0·984	0·085	0·123	1·017	0·100	0·118
0·250	0·984	0·097	0·190	1·015	0·129	0·139
0·183	0·990	0·112	0·280	1·032	0·180	0·160
0·117	1·006	0·155	0·435	1·075	0·277	0·148
0·067	1·015	0·220	0·120	1·080	0·345	+0·020
0·017	1·020	0·255	—0·430	1·075	0·340	—0·120
—0·067	0·972	0·071	—0·330	1·013	0·180	—0·179
—0·167	1·000	0·034	—0·180	1·013	0·055	—0·135
—0·333	1·000	0·018	—0·103	1·013	0·035	—0·099
—0·500	1·000	0·010	—0·078	1·013	0·027	—0·079
—0·833	1·000	0·004	—0·053	1·013	0·019	—0·053
—1·167	1·000	0·003	—0·040	1·013	0·014	—0·037
—1·500	1·000	0·002	—0·032	1·013	0·010	—0·030

y Chords.	$z = -0.238$			$z = -0.388$		
	$-u$	v	w	$-u$	v	w
2·833	1·018	0·004	0·088	0·995	0·006	0·079
2·167	1·018	0·011	0·091	0·995	0·017	0·079
1·667	1·018	0·018	0·093	0·995	0·027	0·079
1·333	1·018	0·027	0·095	0·995	0·034	0·079
1·000	1·018	0·041	0·097	0·998	0·043	0·079
0·833	1·018	0·049	0·098	1·000	0·051	0·078
0·667	1·018	0·061	0·099	1·000	0·061	0·077
0·500	1·018	0·078	0·102	1·002	0·076	0·074
0·417	1·020	0·091	0·103	1·003	0·086	0·071
0·333	1·020	0·112	0·107	1·005	0·099	0·063
0·250	1·024	0·140	0·107	1·006	0·113	0·050
0·183	1·026	0·172	0·098	1·006	0·125	0·033
0·117	1·028	0·210	+0·070	1·008	0·135	+0·013
0·067	1·028	0·245	0	1·008	0·139	—0·001
0·017	1·028	0·230	—0·080	1·008	0·139	—0·015
—0·067	1·030	0·170	—0·120	1·009	0·121	—0·041
—0·167	1·030	0·104	—0·126	1·009	0·098	—0·067
—0·333	1·030	0·054	—0·097	1·009	0·063	—0·068
—0·500	1·030	0·030	—0·074	1·009	0·040	—0·062
—0·833	1·030	0·017	—0·050	1·009	0·023	—0·049
—1·167	1·030	0·012	—0·036	1·009	0·016	—0·037
—1·500	1·030	0·008	—0·027	1·009	0·013	—0·029

TABLE VIII.—Section C (two chords behind trailing edge of aërofoil).   Experimental Results.

y Chords.	$z = 1.225$ Hot-wire			$z = 0.750$ Tube			$z = 0.573$ Hot-wire		
	$-u$	v	w	$-u$	v	w	$-u$	v	w
2.833	1.010	−0.002	0.038	1.000	−0.006	0.050	1.000	−0.002	0.053
2.167	1.010	−0.012	0.036	1.000	−0.016	0.050	1.000	−0.011	0.054
1.667	1.010	−0.020	0.032	1.000	−0.027	0.050	1.000	−0.023	0.055
1.333	1.010	−0.026	0.028	1.000	−0.036	0.050	0.995	−0.032	0.054
1.000	1.010	−0.032	0.021	1.000	−0.048	0.045	0.995	−0.045	0.050
0.833	1.010	−0.036	0.016	1.000	−0.054	0.039	0.995	−0.053	0.046
0.667	1.010	−0.039	0.012	1.000	−0.061	0.031	0.995	−0.062	0.039
0.500	1.010	−0.043	0.007	1.000	−0.067	0.021	0.995	−0.071	0.029
0.400	1.010	−0.045	0.004	1.000	−0.071	0.015	0.995	−0.075	0.022
0.333	1.010	−0.046	+0.002	1.000	−0.072	0.009	0.995	−0.078	0.016
0.267	1.010	−0.047	0	1.000	−0.073	+0.004	0.995	−0.079	0.009
0.217	1.010	−0.047	−0.002	1.000	−0.073	0	0.995	−0.080	+0.004
0.167	1.010	−0.047	−0.004	1.000	−0.073	−0.004	0.995	−0.080	−0.003
0.117	1.010	−0.047	−0.006	1.000	−0.072	−0.009	0.995	−0.081	−0.009
0.067	1.010	−0.047	−0.009	1.000	−0.071	−0.031	0.995	−0.080	−0.015
0	1.010	−0.046	−0.011	1.000	−0.067	−0.019	0.995	−0.077	−0.023
−0.083	1.010	−0.044	−0.014	1.000	−0.063	−0.025	0.995	−0.070	−0.032
−0.167	1.010	−0.042	−0.017	1.000	−0.058	−0.030	1.000	−0.062	−0.039
−0.333	1.010	−0.037	−0.022	1.000	−0.049	−0.037	1.000	−0.048	−0.045
−0.500	1.010	−0.033	−0.026	1.000	−0.041	−0.040	1.000	−0.037	−0.046
−0.833	1.010	−0.024	−0.031	1.000	−0.029	−0.041	1.000	−0.019	−0.041
−1.167	1.010	−0.016	−0.033	1.000	−0.018	−0.039	1.000	−0.009	−0.032
−1.500	1.010	−0.008	−0.033	1.000	−0.010	−0.028	1.000	−0.002	−0.026

y Chords.	$z = 0.297$ Hot-wire			$z = 0.192$ Hot-wire			$z = 0.078$ Hot-wire		
	$-u$	v	w	$-u$	v	w	$-u$	v	w
2.833	1.010	−0.004	0.056	0.997	0	0.054	0.994	0	0.056
2.167	1.010	−0.019	0.056	0.997	−0.011	0.056	0.994	0	0.060
1.667	1.010	−0.028	0.060	0.997	−0.017	0.062	0.994	0.090	0.065
1.333	1.010	−0.039	0.066	0.997	−0.023	0.068	0.994	0.018	0.069
1.000	1.010	−0.056	0.070	0.997	−0.034	0.072	0.994	0.024	0.072
0.833	1.010	−0.067	0.071	0.997	−0.041	0.073	0.994	0.024	0.075
0.667	1.010	−0.082	0.066	0.997	−0.053	0.071	0.996	0.019	0.083
0.500	1.010	−0.103	0.055	0.995	−0.082	0.062	1.006	+0.007	0.094
0.400	1.010	−0.119	0.043	0.993	−0.112	0.049	1.020	−0.010	0.102
0.333	1.010	−0.129	0.030	0.991	−0.130	0.037	1.034	−0.037	0.104
0.267	1.010	−0.136	+0.014	0.992	−0.144	+0.019	1.050	−0.080	0.104
0.217	1.010	−0.140	0	1.001	−0.154	0	1.054	−0.120	0.087
0.167	1.010	−0.140	−0.015	1.013	−0.159	−0.019	1.050	−0.164	+0.036
0.117	1.010	−0.136	−0.029	1.020	−0.159	−0.039	1.037	−0.195	−0.020
0.067	1.010	−0.129	−0.043	1.024	−0.154	−0.057	1.023	−0.187	−0.085
0	1.006	−0.117	−0.059	1.023	−0.137	−0.084	1.008	−0.157	−0.163
−0.083	1.002	−0.099	−0.069	1.003	−0.105	−0.098	1.005	−0.097	−0.163
−0.167	1.004	−0.081	−0.074	1.003	−0.080	−0.098	1.005	−0.063	−0.143
−0.333	1.008	−0.051	−0.072	1.003	−0.045	−0.090	1.005	−0.035	−0.108
−0.500	1.008	−0.033	−0.061	1.003	−0.026	−0.075	1.005	−0.022	−0.083
−0.833	1.008	−0.015	−0.047	1.003	−0.010	−0.052	1.005	−0.010	−0.057
−1.167	1.008	−0.006	−0.036	1.003	−0.005	−0.039	1.005	−0.005	−0.039
−1.500	1.008	−0.004	−0.028	1.003	−0.002	−0.029	1.005	−0.002	−0.029

TABLE VIII—continued.

y Chords.	$z = 0.017$ Hot-wire			$z = -0.030$ Hot-wire and Tube (mean) Comparison given in Fig. 5.			$z = -0.058$ Tube		
	$-u$	v	w	$-u$	v	w	$-u$	v	w
2·833	0·990	0·003	0·054	1·015	0·007	0·064	1·008	0	0·062
2·167	0·990	0·010	0·056	1·015	0·009	0·068	1·008	0·007	0·062
1·667	0·990	0·018	0·060	1·015	0·015	0·070	1·008	0·013	0·065
1·333	0·990	0·023	0·064	1·015	0·023	0·071	1·008	0·019	0·068
1·000	0·990	0·030	0·070	1·015	0·029	0·077	1·008	0·028	0·074
0·833	0·990	0·032	0·074	1·015	0·031	0·081	1·008	0·032	0·079
0·667	0·992	0·029	0·083	1·015	0·031	0·089	1·008	0·033	0·089
0·500	0·994	0·019	0·098	1·015	0·027	0·108	1·008	0·028	0·109
0·400	1·000	+0·005	+0·115	1·020	+0·016	0·139	1·008	0·023	0·132
0·333	1·010	—0·017	0·136	1·020	—0·005	0·196	1·008	0·017	0·158
0·267	1·025	—0·070	0·158	1·025	—0·046	0·233	1·002	+0·007	0·228
0·217	1·045	—0·135	0·157	1·030	—0·164	0·276	1·010	—0·080	0·310
0·167	1·070	—0·215	+0·112	1·025	—0·360	+0·270	1·012	—0·280	+0·400
0·117	1·020	—0·280	—0·020	1·000	—0·440	—0·080	0·970	—0·330	—0·090
0·067	1·004	—0·214	—0·155	1·005	—0·280	—0·304	0·985	—0·210	—0·404
0	0·996	—0·132	—0·191	1·020	—0·100	—0·266	1·008	—0·037	—0·300
—0·083	0·990	—0·080	—0·195	1·005	—0·041	—0·212	0·987	—0·013	—0·220
—0·167	0·990	—0·039	—0·153	1·010	—0·019	—0·166	1·000	—0·007	—0·168
—0·333	0·990	—0·015	—0·107	1·015	—0·007	—0·115	1·007	—0·002	—0·115
—0·500	0·990	—0·009	—0·081	1·015	—0·001	—0·089	1·007	—0·002	—0·089
—0·833	0·990	—0·001	—0·054	1·015	+0·001	—0·055	1·007	—0·001	—0·061
—1·167	0·990	+0·003	—0·041	1·015	0·002	—0·035	1·007	0	—0·047
—1·500	0·990	0·005	—0·031	1·015	0·003	—0·026	1·007	0	—0·038

y Chords.	$z = -0.088$ Hot-wire and Tube (mean) Comparison given in Fig. 5.			$z = -0.115$ Tube			$z = -0.187$ Hot-wire		
	$-u$	v	w	$-u$	v	w	$-u$	v	w
2·833	1·010	0·002	0·054	1·007	0	0·056	0·995	0·004	0·056
2·167	1·010	0·006	0·055	1·007	0·006	0·056	0·995	0·008	0·056
1·667	1·010	0·014	0·056	1·007	0·013	0·059	0·995	0·013	0·059
1·333	1·010	0·021	0·059	1·007	0·020	0·062	0·995	0·019	0·060
1·000	1·010	0·028	0·065	1·007	0·028	0·067	0·995	0·029	0·063
0·833	1·010	0·032	0·072	1·007	0·032	0·073	0·996	0·037	0·069
0·667	1·010	0·035	0·083	1·008	0·037	0·085	0·997	0·047	0·081
0·500	1·010	0·038	0·107	1·013	0·045	0·107	0·998	0·065	0·101
0·400	1·010	0·037	0·134	1·014	0·053	0·133	0·999	0·083	0·120
0·333	1·010	0·036	0·167	1·012	0·065	0·165	0·999	0·106	0·140
0·267	1·015	0·031	0·240	1·008	0·085	0·230	0·999	0·150	0·171
0·217	1·020	0·025	0·330	1·002	0·130	0·310	0·999	0·200	0·178
0·167	1·050	+0·005	+0·460	0·996	0·270	+0·360	0·999	0·290	0·140
0·117	1·040	—0·220	—0·020	1·010	0·446	—0·020	0·999	0·310	+0·015
0·067	1·040	+0·050	—0·460	1·028	0·320	—0·360	0·999	0·305	—0·120
0	1·040	0·027	—0·320	1·010	0·110	—0·305	0·999	0·220	—0·200
—0·083	1·015	0·017	—0·228	1·002	0·048	—0·222	1·000	0·106	—0·187
—0·167	1·010	0·011	—0·172	1·006	0·026	—0·165	1·002	0·059	—0·150
—0·333	1·010	0·003	—0·116	1·006	0·011	—0·115	1·004	0·029	—0·106
—0·500	1·010	0	—0·089	1·006	0·003	—0·088	1·004	0·017	—0·081
—0·833	1·010	0	—0·059	1·006	0	—0·056	1·005	0·010	—0·054
—1·167	1·010	0	—0·045	1·006	0	—0·041	1·005	0·008	—0·040
—1·500	1·010	0	—0·039	1·006	0	—0·037	1·005	0·006	—0·029

TABLE VIII—*continued.*

y Chords.	z = −0·210 Hot-wire and Tube (mean) Comparison given in Fig. 5.			z = −0·350 Hot-wire			Z = −0·530 Hot-wire		
	−u	v	w	−u	v	w	−u	v	w
2·833	1·005	0·003	0·054	1·007	0·002	0·053	1·005	0·004	0·055
2·167	1·005	0·008	0·054	1·007	0·010	0·054	1·005	0·012	0·055
1·667	1·005	0·015	0·060	1·007	0·016	0·054	1·005	0·020	0·055
1·333	1·005	0·021	0·063	1·007	0·023	0·056	1·005	0·028	0·055
1·000	1·005	0·029	0·067	1·007	0·033	0·061	1·005	0·039	0·056
0·833	1·005	0·036	0·071	1·007	0·042	0·064	1·005	0·047	0·056
0·667	1·005	0·047	0·077	1·007	0·055	0·067	1·005	0·061	0·056
0·500	1·005	0·064	0·094	1·007	0·074	0·073	1·005	0·079	0·049
0·400	1·005	0·085	0·112	1·010	0·091	0·074	1·005	0·090	0·043
0·333	1·000	0·110	0·129	1·019	0·106	0·073	1·005	0·097	0·037
0·267	1·000	0·150	0·143	1·022	0·123	0·065	1·005	0·103	0·027
0·217	0·995	0·190	0·147	1·018	0·144	0·050	1·005	0·107	0·019
0·167	0·990	0·275	0·103	1·013	0·168	0·030	1·005	0·110	+0·009
0·117	0·990	0·310	+0·020	1·008	0·179	+0·004	1·005	0·111	−0·002
0·067	0·995	0·275	−0·080	1·005	0·177	−0·030	1·005	0·110	−0·013
0	1·005	0·205	−0·175	1·003	0·159	−0·076	1·000	0·106	−0·029
−0·083	1·000	0·124	−0·169	1·005	0·123	−0·093	1·000	0·097	−0·042
−0·167	1·000	0·072	−0·143	1·013	0·092	−0·094	1·003	0·085	−0·049
−0·333	1·000	0·032	−0·105	1·013	0·051	−0·089	1·003	0·063	−0·056
−0·500	1·000	0·020	−0·079	1·013	0·032	−0·079	1·005	0·043	−0·058
−0·833	1·000	0·010	−0·054	1·013	0·016	−0·057	1·008	0·024	−0·051
−1·167	1·000	0·005	−0·044	1·013	0·012	−0·046	1·010	0·015	−0·038
−1·500	1·000	0·003	−0·038	1·013	0·011	−0·039	1·010	0·012	−0·028

y Chords.	z = −1·01 Hot-wire			z = −1·333 Hot-wire		
	−u	v	w	−u	v	w
2·833	1·000	0·003	0·043	1·007	0	0·043
2·167	1·000	0·012	0·043	1·007	0·007	0·042
1·667	1·000	0·022	0·043	1·007	0·017	0·040
1·333	1·000	0·030	0·043	1·007	0·023	0·036
1·000	1·008	0·038	0·039	1·007	0·028	0·031
0·833	1·008	0·043	0·036	1·007	0·030	0·028
0·667	1·008	0·047	0·030	1·007	0·033	0·023
0·500	1·009	0·051	0·023	1·007	0·037	0·017
0·400	1·009	0·054	0·018	1·007	0·038	0·014
0·333	1·010	0·056	0·015	1·007	0·039	0·011
0·267	1·010	0·057	0·011	1·007	0·040	0·009
0·217	1·010	0·057	0·008	1·007	0·040	0·007
0·167	1·009	0·057	0·005	1·007	0·040	0·004
0·177	1·006	0·057	0·002	1·007	0·040	+0·002
0·067	1·004	0·056	0	1·007	0·039	0
0	1·003	0·054	−0·005	1·007	0·039	−0·003
−0·083	1·004	0·052	−0·011	1·007	0·038	−0·007
−0·167	1·008	0·049	−0·016	1·007	0·037	−0·011
−0·333	1·008	0·043	−0·023	1·007	0·035	−0·017
−0·500	1·008	0·038	−0·027	1·007	0·033	−0·021
−0·833	1·010	0·028	−0·028	1·007	0·028	−0·026
−1·167	1·010	0·025	−0·028	1·007	0·024	−0·027
−1·500	1·010	0·021	−0·027	1·007	0·019	−0·027

TABLE IX.—Section D (13 chords behind trailing edge of aërofoil).   Experimental Results.   (Hot-wire.)

y Chords.	$z = +0.483$			$z = +0.278$			$z = +0.147$		
	$-u$	v	w	$-u$	v	w	$-u$	v	w
2·833	1·000	0·006	0·048	1·012	0	0·041	0·992	0·001	0·038
2·167	1·000	0·004	0·050	1·012	0	0·046	0·992	0·002	0·039
1·667	1·000	+0·001	0·053	1·012	0	0·051	0·992	0·002	0·040
1·333	1·000	−0·003	0·057	1·012	−0·005	0·057	0·996	+0·001	0·047
1·000	1·000	−0·017	0·061	1·012	−0·019	0·067	1·000	−0·007	0·062
0·750	1·000	−0·036	0·056	1·012	−0·040	0·074	1·000	−0·026	0·082
0·600	1·000	−0·054	0·048	1·012	−0·065	0·075	1·005	−0·048	0·096
0·483	1·000	−0·068	0·036	1·012	−0·093	0·064	1·010	−0·084	0·098
0·383	1·002	−0·074	0·016	1·017	−0·116	0·042	1·025	−0·145	0·078
0·317	1·006	−0·076	+0·003	1·012	−0·124	+0·010	1·040	−0·186	+0·030
0·267	1·009	−0·076	−0·006	1·008	−0·125	−0·011	1·044	−0·191	−0·012
0·217	1·007	−0·076	−0·015	1·008	−0·119	−0·028	1·040	−0·190	−0·040
0·150	1·005	−0·073	−0·027	1·011	−0·101	−0·049	1·033	−0·172	−0·086
0·067	1·005	−0·070	−0·043	1·020	−0·085	−0·066	1·024	−0·109	−0·113
−0·067	1·000	−0·063	−0·066	1·024	−0·063	−0·081	1·014	−0·061	−0·113
−0·250	1·000	−0·042	−0·069	1·024	−0·043	−0·093	1·010	−0·039	−0·106
−0·500	1·000	−0·026	−0·067	1·024	−0·024	−0·077	1·010	−0·021	−0·090
−0·833	1·000	−0·017	−0·057	1·024	−0·012	−0·060	1·010	−0·011	−0·070
−1·167	1·000	−0·011	−0·040	1·024	−0·008	−0·046	1·010	−0·005	−0·053
−1·500	1·000	−0·005	−0·030	1·024	−0·005	−0·036	1·010	−0·001	−0·039

y Chords.	$z = +0.007$			$z = -0.022$			$z = -0.055$		
	$-u$	v	w	$-u$	v	w	$-u$	v	w
2·833	0·984	0·006	0·039	0·997	0·004	0·044	1·010	0·003	0·045
2·167	0·984	0·007	0·042	0·997	0·009	0·052	1·010	0·006	0·051
1·667	0·984	0·007	0·050	0·997	0·012	0·061	1·010	0·009	0·055
1·333	0·984	0·008	0·059	0·997	0·012	0·068	1·010	0·010	0·061
1·000	0·984	+0·006	0·070	0·997	0·008	0·080	1·010	0·013	0·079
0·750	0·984	−0·010	0·095	0·997	+0·002	0·105	1·010	0·012	0·110
0·600	0·984	−0·029	0·128	0·997	−0·004	0·139	1·030	0·010	0·145
0·483	0·987	−0·056	0·163	1·000	−0·017	0·178	1·040	+0·006	0·190
0·383	0·990	−0·101	0·194	1·020	−0·060	0·232	1·040	−0·005	0·240
0·317	1·000	−0·154	+0·228	1·032	−0·135	+0·234	1·020	−0·026	+0·262
0·267	1·010	−0·305	{+0·130} {+0·230}	1·034	−0·373	−0·016	0·980	−0·375	−0·100
0·217	1·030	−0·284	−0·230	1·032	−0·200	−0·200	0·995	−0·080	−0·345
0·150	1·090	−0·140	−0·225	1·028	−0·064	−0·239	1·016	+0·016	−0·265
0·067	—	−0·050	−0·193	1·019	−0·024	−0·197	1·015	0·015	−0·200
−0·067	0·972	−0·019	−0·150	1·010	−0·008	−0·148	1·010	0·012	−0·141
−0·250	0·990	−0·006	−0·111	1·010	+0·002	−0·113	1·012	0·010	−0·116
−0·500	0·992	−0·001	−0·082	1·013	+0·002	−0·085	1·012	0·009	−0·089
−0·833	0·992	0	−0·061	1·016	0	−0·060	1·012	0·006	−0·064
−1·167	0·992	0	−0·047	1·016	0	−0·044	1·012	0·004	−0·047
−1·500	0·992	0	−0·038	1·016	0	−0·034	1·012	0·002	−0·035

TABLE IX—*continued.*

y Chords.	$z = -0.088$			$z = -0.113$			$z = -0.138$		
	$-u$	v	w	$-u$	v	w	$-u$	v	w
2·833	0·990	0·004	0·042	1·000	0·005	0·042	1·003	0·002	0·043
2·167	0·990	0·009	0·046	1·000	0·009	0·048	1·003	0·003	0·046
1·667	0·990	0·013	0·052	1·000	0·011	0·053	1·003	0·005	0·052
1·333	0·990	0·015	0·061	1·000	0·013	0·060	1·003	0·007	0·057
1·000	0·990	0·018	0·079	1·000	0·015	0·075	1·003	0·011	0·075
0·750	0·990	0·021	0·106	1·000	0·025	0·109	1·003	0·020	0·100
0·600	0·990	0·025	0·137	1·000	0·030	0·140	0·996	0·036	0·128
0·483	0·994	0·037	0·183	1·027	0·043	0·180	0·993	0·063	0·160
0·383	1·017	0·063	0·250	—	0·070	—	1·050	0·110	0·200
0·317	1·080	0·089	+0·255	1·060	0·101	+0·220	1·073	0·180	+0·233
0·267	1·050	$\begin{cases}+0·091\\-0·015\end{cases}$	—0·175	1·046	0·142	$\begin{cases}-0·140\\-0·310\end{cases}$	1·054	—	—0·020
0·217	1·035	0·086	—0·370	1·037	0·116	—0·350	1·043	0·190	—0·286
0·150	1·024	0·058	—0·265	1·028	0·078	—0·254	1·030	0·135	—0·234
0·067	1·015	0·038	—0·187	1·020	0·055	—0·201	1·017	0·082	—0·183
—0·067	1·000	0·023	—0·140	1·013	0·037	—0·149	1·000	0·039	—0·138
—0·250	1·000	0·015	—0·107	1·000	0·024	—0·110	1·000	0·023	—0·111
—0·500	1·000	0·008	—0·079	1·000	0·015	—0·082	1·003	0·013	—0·086
—0·833	1·000	0·003	—0·054	1·000	0·009	—0·054	1·006	0·005	—0·059
—1·167	1·000	0·001	—0·040	1·000	0·006	—0·037	1·010	0·001	—0·042
—1·500	1·000	0	—0·034	1·000	0·004	—0·027	1·014	0	—0·035

y Chords.	$z = -0.240$			$z = -0.350$			$z = -0.577$		
	$-u$	v	w	$-u$	v	w	$-u$	v	w
2·833	1·020	0	0·041	0·986	0·006	0·044	0·990	0·006	0·041
2·167	1·020	0·005	0·044	0·986	0·013	0·049	0·990	0·012	0·045
1·667	1·020	0·009	0·047	0·990	0·018	0·053	0·992	0·018	0·050
1·333	1·020	0·010	0·050	0·990	0·021	0·057	0·996	0·025	0·052
1·000	1·020	0·014	0·065	0·990	0·027	0·068	0·998	0·038	0·055
0·750	1·020	0·032	0·083	0·990	0·053	0·083	1·004	0·057	0·055
0·600	1·024	0·061	0·099	0·990	0·080	0·091	1·010	0·072	0·052
0·483	1·021	0·099	0·116	0·990	0·106	0·083	1·017	0·087	0·044
0·383	1·022	0·144	0·124	0·996	0·134	0·061	0·996	0·101	0·026
0·317	1·080	0·190	0·100	0·998	0·156	0·039	0·996	0·108	+0·011
0·267	1·084	0·210	+0·050	1·001	0·162	+0·009	0·996	0·109	—0·001
0·217	1·084	0·211	—0·035	1·000	0·161	—0·022	0·998	0·110	—0·013
0·150	1·075	0·176	—0·128	0·998	0·147	—0·050	1·000	0·107	—0·026
0·067	1·010	0·118	—0·142	0·996	0·124	—0·078	1·000	0·100	—0·039
—0·067	1·005	0·073	—0·139	0·992	0·086	—0·100	1·003	0·085	—0·056
—0·250	1·010	0·048	—0·119	0·996	0·053	—0·089	1·003	0·059	—0·058
—0·500	1·017	0·026	—0·095	1·000	0·029	—0·071	1·003	0·038	—0·055
—0·833	1·017	0·011	—0·071	1·000	0·017	—0·048	1·003	0·026	—0·047
—1·167	1·017	0·006	—0·055	1·003	0·010	—0·034	0·990	0·018	—0·035
—1·500	1·017	0·003	—0·050	1·005	0·007	—0·027	0·980	0·013	—0·023

Scale of Inches
1 2 3 4

FIG. 2.